Tryptophan-Derived Metabolites Are Required for Antifungal Defense in the Arabidopsis *mlo2* Mutant[1][C][W][OA]

Chiara Consonni, Paweł Bednarek, Matt Humphry, Fedra Francocci, Simone Ferrari, Anne Harzen, Emiel Ver Loren van Themaat, and Ralph Panstruga*

Department of Plant-Microbe Interactions (C.C., P.B., M.H., E.V.L.v.T., R.P.) and Mass Spectrometry Group (A.H.), Max-Planck Institute for Plant Breeding Research, D–50829 Cologne, Germany; and Dipartimento di Biologia Vegetale, Sapienza Università di Roma, 00185 Rome, Italy (F.F., S.F.)

Arabidopsis (*Arabidopsis thaliana*) genes *MILDEW RESISTANCE LOCUS O2* (*MLO2*), *MLO6*, and *MLO12* exhibit unequal genetic redundancy with respect to the modulation of defense responses against powdery mildew fungi and the control of developmental phenotypes such as premature leaf decay. We show that early chlorosis and necrosis of rosette leaves in *mlo2 mlo6 mlo12* mutants reflects an authentic but untimely leaf senescence program. Comparative transcriptional profiling revealed that transcripts of several genes encoding tryptophan biosynthetic and metabolic enzymes hyperaccumulate during vegetative development in the *mlo2 mlo6 mlo12* mutant. Elevated expression levels of these genes correlate with altered steady-state levels of several indolic metabolites, including the phytoalexin camalexin and indolic glucosinolates, during development in the *mlo2* single mutant and the *mlo2 mlo6 mlo12* triple mutant. Results of genetic epistasis analysis suggest a decisive role for indolic metabolites in *mlo2*-conditioned antifungal defense against both biotrophic powdery mildews and a camalexin-sensitive strain of the necrotrophic fungus *Botrytis cinerea*. The wound- and pathogen-responsive callose synthase POWDERY MILDEW RESISTANCE4/GLUCAN SYNTHASE-LIKE5 was found to be responsible for the spontaneous callose deposits in *mlo2* mutant plants but dispensable for *mlo2*-conditioned penetration resistance. Our data strengthen the notion that powdery mildew resistance of *mlo2* genotypes is based on the same defense execution machinery as innate antifungal immune responses that restrict the invasion of nonadapted fungal pathogens.

Powdery mildews represent a group of widespread ascomycete phytopathogens that can colonize a broad range of angiosperm plant species. Attempted fungal penetration into epidermal host cells triggers multifaceted plant defense-related responses, such as the transcriptional activation of *PATHOGENESIS-RELATED* (*PR*) genes, de novo cell wall biosynthesis underneath fungal contact sites (papillae), as well the biosynthesis and local extrusion of antimicrobial molecules (for review, see Eichmann and Hückelhoven, 2008). The toxic principles that ultimately cause abortion of fungal pathogenesis, however, remain largely enigmatic.

Pathogen-induced plant secondary metabolites with antimicrobial activity, also known as phytoalexins, are low M_r compounds that are structurally diverse and often restricted in their occurrence to a limited number of plant species (Glawischnig, 2007). At present, the only phytoalexin known in Arabidopsis (*Arabidopsis thaliana*) is the indole derivative 3-thiazol-2′-yl-indole, also known as camalexin (Tsuji et al., 1992). Camalexin is derived from indole-3-acetaldoxime (Glawischnig et al., 2004), which in turn is synthesized from Trp by the functionally redundant CYTOCHROME P450 monooxygenases CYP79B2 and CYP79B3 (Hull et al., 2000; Mikkelsen et al., 2000). The reaction catalyzed by CYP79B2 and CYP79B3 is the sole entry point for a range of biosynthetic pathways leading to diverse indolic metabolites, including camalexin and indole glucosinolates (1-thio-β-D-glucosides; Supplemental Fig. S1). Consistently, *cyp79B2 cyp79B3* double mutant plants are unable to accumulate these metabolites (Zhao et al., 2002; Glawischnig et al., 2004).

In a genetic screen for camalexin-deficient mutants, *phytoalexin deficient3* (*pad3*) was isolated (Glazebrook and Ausubel, 1994) and subsequently shown to be defective in another cytochrome P450 enzyme, CYP71B15, which catalyzes the final step of camalexin

[1] This work was supported by the Deutsche Forschungsgemeinschaft (grant no. PA861/4) and the Max-Planck Society to R.P. and by a postdoctoral fellowship from the Alexander von Humboldt Foundation to M.H.

* Corresponding author; e-mail panstrug@mpiz-koeln.mpg.de.

The author responsible for distribution of materials integral to the findings presented in this article in accordance with the policy described in the Instructions for Authors (www.plantphysiol.org) is: Ralph Panstruga (panstrug@mpiz-koeln.mpg.de).

[C] Some figures in this article are displayed in color online but in black and white in the print edition.

[W] The online version of this article contains Web-only data.

[OA] Open Access articles can be viewed online without a subscription.

www.plantphysiol.org/cgi/doi/10.1104/pp.109.147660

biosynthesis (Zhou et al., 1999; Schuhegger et al., 2006; Supplemental Fig. S1). *pad3* mutants have been extensively used to study the role of camalexin in plant-pathogen interactions, leading to the proposition that camalexin contributes to resistance against necrotrophic pathogens but not against biotrophs (for review, see Glazebrook, 2005). For instance, attack by the powdery mildew fungus *Golovinomyces orontii*, one of several powdery mildew species that are virulent on Arabidopsis (Micali et al., 2008), does not trigger camalexin accumulation, and *pad3* mutants do not exhibit enhanced susceptibility at the macroscopic level (Reuber et al., 1998).

In barley (*Hordeum vulgare*) and Arabidopsis, penetration attempts of powdery mildew fungi typically induce the localized formation of callose-containing cell wall appositions (papillae; Aist, 1976; Zeyen et al., 2002). Callose is a polymeric (1→3)-β-D-glucan that is synthesized by plasma membrane-resident GLUCAN SYNTHASE-LIKE (GSL) proteins. Callose deposition in papillae has been implicated in the highly efficient powdery mildew resistance of barley *mildew resistance locus o* (*mlo*) mutants, supposedly by contributing as a physical barrier to impede fungal entry into host cells (Skou, 1982, 1985; Bayles et al., 1990). However, recent genetic studies in Arabidopsis challenged a decisive role for papillary callose in antifungal defense. The *POWDERY MILDEW RESISTANT4* (*PMR4*) gene, originally identified in a genetic screen for Arabidopsis mutants that are resistant to adapted powdery mildews, was found to encode GSL5. In rosette leaves, GSL5-generated callose is primarily deposited at wound sites and in pathogen-triggered papillae, suggesting that a lack of callose deposition in papillae does not compromise antifungal defense (Jacobs et al., 2003; Nishimura et al., 2003).

In the genetic screen leading to the identification of *pmr4*, further *pmr* mutants were isolated (Vogel and Somerville, 2000). One of these is defective in *PMR2*, which is allelic to *MLO2*, encoding a member of the seven-transmembrane-domain MLO protein family (Devoto et al., 2003). Mutant versions of the founder of this protein family, barley Mlo, are known to confer broad-spectrum resistance to powdery mildew fungi (Jørgensen, 1992; Büschges et al., 1997). Arabidopsis MLO2 and its closest homologs, MLO6 and MLO12, were found to be required for full susceptibility against powdery mildews in Arabidopsis (Consonni et al., 2006). While mutations in *MLO2* alone confer partial resistance against *G. orontii* and *Golovinomyces cichoracearum*, additional mutations in *MLO6* and *MLO12* resulted in full immunity, which is characterized by early termination of fungal pathogenesis before successful penetration of the host cell wall (Consonni et al., 2006). This infection phenotype is reminiscent of fully resistant barley *mlo* single mutants. Collectively, these findings suggest that distantly related powdery mildew species rely on functionally conserved host proteins in dicot and monocot plants for successful pathogenesis (Panstruga, 2005).

Partial *mlo2* resistance in Arabidopsis depends on three *PENETRATION* (*PEN*) genes that were originally discovered based on their requirement for effective extracellular defense responses against the nonadapted powdery mildews *Blumeria graminis* f. sp. *hordei* and *Erysiphe pisi* (Collins et al., 2003; Lipka et al., 2005; Stein et al., 2006). *PEN1* encodes a plasma membrane-resident syntaxin (t-SNARE) involved in exocytosis (Collins et al., 2003; Kwon et al., 2008). *PEN2* codes for an atypical myrosinase (Bednarek et al., 2009) and cofunctions with the plasma membrane-resident PEN3 ATP-binding cassette multidrug transporter in a parallel extracellular defense pathway, presumably by targeted delivery of indole glucosinolate-derived antimicrobial metabolites into the apoplastic space (Lipka et al., 2005; Stein et al., 2006; Bednarek et al., 2009). Besides their supposed antimicrobial capacity, indolic glucosinolates may have an additional role as signaling molecules during innate immune responses (Clay et al., 2009).

Mutations in *MLO* genes result not only in resistance against powdery mildew fungi but also in additional, developmentally controlled pleiotropic phenotypes. Spontaneous accumulation of callose in leaf mesophyll cells and early leaf chlorosis/necrosis that is reminiscent of senescence was observed both in barley and Arabidopsis *mlo* mutants (Wolter et al., 1993; Piffanelli et al., 2002; Consonni et al., 2006). In Arabidopsis, this phenotype is fully dependent on salicylic acid (SA) accumulation but independent of jasmonic acid (JA) and ethylene (ET) biosynthesis and signaling (Consonni et al., 2006), demonstrating separate requirements for the desired disease resistance trait and undesired leaf chlorosis/necrosis in *mlo* mutant plants.

Here, we employed comparative global gene expression analysis and performed targeted metabolite profiling to obtain deeper insights into the molecular basis of the pleiotropic phenotypes in the Arabidopsis *mlo2* single mutant and *mlo2 mlo6 mlo12* triple mutant. We found aberrant accumulation patterns of indolic secondary metabolites in the single and triple mutants during the appearance of the *mlo2*-conditioned early leaf senescence phenotype. Genetic analysis revealed a critical contribution of indolics, including camalexin and glucosinolates, in *mlo2*-mediated resistance.

RESULTS

Developmentally Controlled Leaf Chlorosis and Necrosis Reflects Early Senescence of *mlo2* Mutants

We recently reported that Arabidopsis *mlo2* mutants, like barley *mlo* mutants, exhibit a developmentally determined phenotype resembling early leaf senescence. This phenotype is exacerbated in the *mlo2 mlo6 mlo12* triple mutant (Consonni et al., 2006) and varies in the timing of occurrence depending on growth conditions: although plants grown in long

days (16 h of light) start to show leaf chlorosis and necrosis at around 6 weeks after sowing, this appearance arises considerably later (from 9 weeks onward) in plants grown in short-day conditions (10 h of light; data not shown).

To find out whether this phenotype is an authentic senescence process, we measured plant photosynthetic performance (photochemical efficiency of PSII [F_v/F_m]) to assess functional leaf longevity (Maxwell and Johnson, 2000; Oh et al., 2003; Kusaba et al., 2007). The F_v/F_m ratio reflects the quantity of light energy absorbed by PSII that is used for photosynthesis (photochemical efficiency). The optimal value for this parameter is expected to be around 0.83 for leaves of young and healthy plants and decreases with plant age, owing to senescence (Woo et al., 2001; Kim et al., 2006). Photosynthetic performance was measured on defined rosette leaves (leaf 7) of intact plants every 2 to 6 d starting from 24 d after sowing until day 46, corresponding to a rosette of 50% final size (growth stage 3.50) to midflowering (growth stage 6.50; Boyes et al., 2001), respectively. Excellent photosynthetic performance ($F_v/F_m > 0.8$) was observed for both wild-type and *mlo2 mlo6 mlo12* plants at the beginning of the time course (24–38 d; Fig. 1A; Supplemental Fig. S2A), indicating that photochemical efficiency is not constitutively impaired in the *mlo* triple mutant. From day 40 onward, the F_v/F_m ratio declined in both genotypes, although somewhat faster in the *mlo2 mlo6 mlo12* triple mutant (Fig. 1A; Supplemental Fig. S2A). However, this difference was not statistically significant.

We determined the chlorophyll content in ecotype Columbia (Col-0) wild type and *mlo2 mlo6 mlo12* mutant plants throughout development by processing the same leaves that were used for measuring photosynthetic performance. Chlorophyll levels continuously decreased from day 28 onward in both wild-type and mutant plants. However, chlorophyll decay occurred faster in *mlo2 mlo6 mlo12* compared with the wild type, signifying accelerated chlorophyll catabolism in the *mlo* triple mutant (Fig. 1B; Supplemental Fig. S2B). Taken together, these results reveal that typical senescence-associated physiological markers such as photosynthetic performance and chlorophyll content exhibit a trend toward a more rapid decline in the *mlo2 mlo6 mlo12* triple mutant, suggesting that *mlo*-conditioned leaf chlorosis and necrosis in Arabidopsis might be mechanistically related or identical to leaf senescence.

A developmental program that, despite some differences, largely phenocopies the authentic senescence processes of intact plants in time lapse is induced upon placing detached leaves in the dark (so-called dark-induced senescence; Weaver and Amasino, 2001). In comparison with natural senescence, this procedure has the advantage that the initiation of senescence is synchronized among individuals and genotypes. Thus, to further test whether the early leaf chlorosis and necrosis of *mlo* mutants resembles genuine senescence, we comparatively analyzed natural whole plant development and artificial dark-induced senescence of detached leaves in Col-0 wild-type, *mlo2* single mutant, and *mlo2 mlo6 mlo12* triple mutant plants. At the whole plant level, 7-week-old *mlo2* mutants showed the previously reported early leaf chlorosis and necrosis that is exacerbated in *mlo2 mlo6 mlo12* plants (Consonni et al., 2006; Fig. 1C, top row). To trigger dark-induced senescence, the fifth leaf of 4-week-old plants grown in long-day conditions was detached and kept in the dark at 22°C. After 4 d of incubation, leaves of Col-0 plants were still largely green, while leaves of the *mlo2* single mutant and *mlo2 mlo6 mlo12* triple mutant plants exhibited mild and variable (*mlo2*) or pronounced and consistent (*mlo2 mlo6 mlo12*) chlorosis (Fig. 1C, bottom row; see also Figs. 4B and 6C below). This finding further strengthens the notion that the *mlo2*-associated phenotype represents authentic but untimely leaf senescence and in addition provides further support for accelerated progression of the senescence process in the *mlo2* and *mlo2 mlo6 mlo12* mutants.

Transcript Accumulation of *MLO2* Peaks around the Onset of Leaf Senescence

The expression pattern of Arabidopsis *MLO* genes, including *MLO2*, was recently studied by compiling data from transgenic promoter::*GUS* reporter lines, reverse transcription (RT)-PCR analysis, and publicly accessible microarray experiments (Chen et al., 2006). To expand this work, we used a transgenic line harboring an *MLO2* promoter::*GUS* reporter gene construct to temporally and spatially resolve *MLO2* promoter-driven gene expression during vegetative development of Arabidopsis plants grown in short-day (10 h of light) conditions. At 3 weeks after sowing, we observed GUS activity predominantly in the cotyledons and the margins of rosette leaves (Fig. 2A). Intensity and coverage of GUS staining in rosette leaves increased with leaf and plant age, peaking in 6-week-old plants, approximately around the onset of spontaneous callose deposition in the *mlo2* mutant (Consonni et al., 2006). Thereafter, we noted an overall slight decrease in GUS staining intensity. Consistent with publicly accessible microarray data (Schmid et al., 2005; Winter et al., 2007), younger rosette leaves consistently showed less GUS staining throughout vegetative development than older leaves (Fig. 2). In sum, these findings are reminiscent of the observed kinetics of *Mlo* transcript accumulation in barley (Piffanelli et al., 2002) and corroborate a potential functional role for these monocot and dicot Mlo orthologs in senescence-associated physiology.

Transcriptomic Approaches to Unravel the Molecular Basis of *mlo*-Associated Pleiotropic Phenotypes

To gain further knowledge on the molecular mechanisms that underlie the untimely leaf senescence

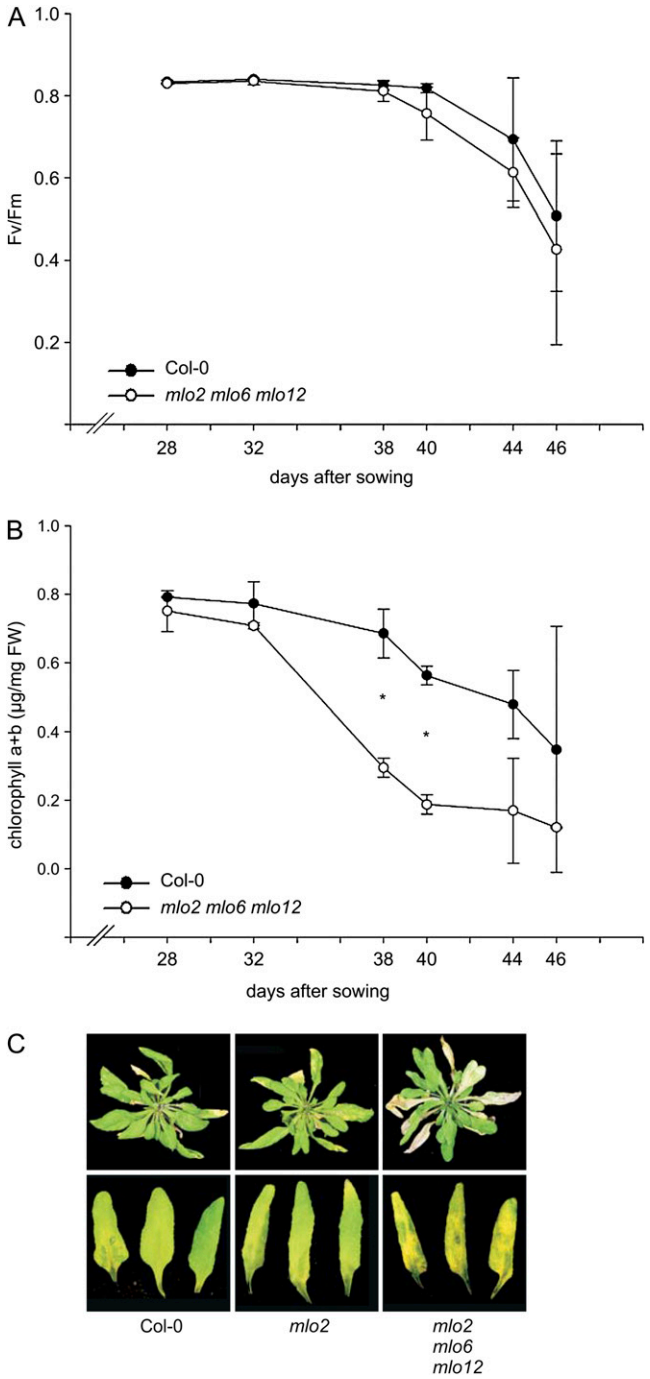

Figure 1. Developmentally controlled *mlo2*-associated leaf chlorosis and necrosis resembles an authentic leaf senescence program. A, Time-course analysis of photosynthetic performance (F_v/F_m) of Col-0 wild-type (black circles) and *mlo2 mlo6 mlo12* (white circles) mutant plants. Data represent means ± SD of four independent rosette leaves (leaf 7) measured at the time points indicated (days after sowing). Plants were grown in long-day conditions. The experiment was repeated twice with similar results (Supplemental Fig. S2; data not shown). B, Time-course analysis of chlorophyll content in leaves of Col-0 wild-type (black circles) and *mlo2 mlo6 mlo12* (white circles) mutant plants. Data represent means ± SD of two independent rosette leaves (leaf 7) collected at the time points indicated (days after sowing) and measured with three technical replicates. Plants were grown in long-day conditions. Note that the very same leaves were taken for measuring chlorophyll content and for determining photosynthetic performance. The experiment was repeated once with similar results (Supplemental Fig. S2). FW, Fresh weight. Asterisks denote statistically significant differences ($P < 0.05$; Student's *t* test) from the Col-0 wild type. C, Habitus of representative unchallenged (pathogen-free) plants at 7 weeks after sowing (top row) and macroscopic phenotypes of detached leaves (leaf 5) from 4-week-old plants dark treated for 4 d (bottom row). Plants were grown in long-day conditions. The experiment was repeated four times with similar results.

phenotype of the *mlo2 mlo6 mlo12* mutant, we performed global gene expression profiling of leaf material collected at different developmental stages using Affymetrix ATH1 GeneChips. Spontaneous callose deposition is a convenient marker for the onset of *mlo*-conditioned leaf senescence and was observed from 6 weeks onward in healthy plants grown in short-day conditions (10 h of light; Consonni et al., 2006). Therefore, we collected mature rosette leaves from unchallenged wild-type and triple mutant plants at 5, 6, and 7 weeks after sowing, signifying time points before (5 weeks), at (6 weeks), and after (7 weeks) the onset of spontaneous callose deposition in the mutant. During this time period, no other signatures of leaf senescence, such as chlorosis and necrosis, were visible in the wild type or the *mlo* triple mutant. Total RNAs extracted from these leaves were labeled with fluorescent dyes and employed in a single hybridization experiment using Affymetrix ATH1 oligonucleotide arrays (for details, see "Materials and Methods").

Consistent with the occurrence of callose deposits at 6 and 7 weeks, unsupervised clustering of the six data sets showed that transcript accumulation in leaves of wild-type and *mlo2 mlo6 mlo12* mutant plants was most similar in 5-week-old plants and exhibited increasing differences in 6- and 7-week-old plants (Supplemental Fig. S3). We analyzed the data to identify candidate genes that exhibit differential transcript levels between wild-type and mutant plants during the developmental period considered. Based on two distinct computational approaches, we generated two result lists, one sorting all 22,810 genes (list A) and the other representing a set of 98 selected genes (list B; Supplemental Table S1). List A is focused on genes more highly expressed in the mutant compared with the wild-type plants when comparing weeks 6 and 7 with week 5. For list B, only those genes were selected with elevated transcript levels specific to the mutant plants at week 7 compared with week 5, while making sure fold changes and absolute intensities are high (for details about the selection criteria and computation procedure, see "Materials and Methods").

In list B as well as in the top approximately 120 genes of list A, we noted a high prevalence of genes whose products are related to the biosynthesis of Trp and Trp-derived (indolic) metabolites. Consistently,

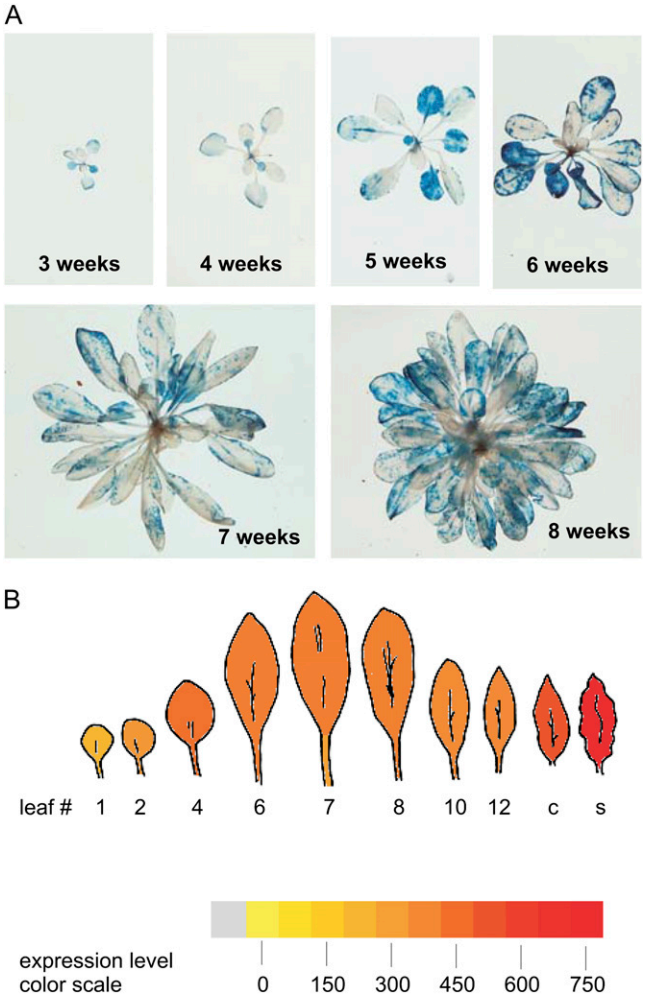

Figure 2. Transcript accumulation of *MLO2* peaks around the onset of leaf senescence. A, Time-course analysis of *MLO2* promoter-driven *GUS* expression in a transgenic Col-0 wild-type plant during vegetative development. Plants were grown in short-day conditions (10 h of light), and entire plants of the indicated ages were stained for GUS activity. The photographs depict exemplary plants from one experiment; similar results were obtained in two independent replicate experiments. B, Schematic representation of *AtMLO2* expression data on publicly accessible microarray databases. The cartoon represents leaves at various developmental stages, color coded with the respective *AtMLO2* expression level (according to the reference color bar shown at the bottom). Microarray source data are from the AtGenExpress project (Schmid et al., 2005). The pictograph is a screenshot from the Arabidopsis eFP browser (http://bbc.botany.utoronto.ca/efp/cgi-bin/efpWeb.cgi; Winter et al., 2007). c, Cauline leaf; s, senescent leaf.

we found a significant enrichment of genes with the Gene Ontology (GO) term "indole derivative biosynthetic process" in list A (adjusted $P = 0.009$) and in list B ($P = 0.03$; for details about the calculation procedure, see "Materials and Methods"). With respect to Trp biosynthesis, these comprised the genes encoding the anthranilate synthase ASA1, phosphoribosylanthranilate transferase (PAT1), the Trp synthase α-subunit TSA1, and indole-3-glycerol phosphate synthase (IGPS). With regard to indole/camalexin/glucosinolate biosynthesis, the genes encoding the cytochrome P450 monooxygenases CYP79B2, CYP71B15/PAD3, CYP71A13, CYP81F2, and CYP83B1 as well as the sulfotransferase SOT16 and the UDP-glucosyltransferase UGT74B1 were included. Finally, the transcription factor MYB51, a key regulator of the genes encoding indole glucosinolate biosynthesis enzymes (Gigolashvili et al., 2007), was found in the top of list A (Table I; Supplemental Table S1). Together, these findings indicate a potential role for indolic secondary metabolites in the *mlo2*-associated deregulated leaf senescence phenotype. Among the identified genes in list B, two are known to be specifically related to early leaf senescence (*WRKY53* and *SAG13*; Lohman et al., 1994; Hinderhofer and Zentgraf, 2001; Miao et al., 2004), suggesting that a senescence-related process might have become initiated in the *mlo2 mlo6 mlo12* mutant but not yet in wild-type plants (Table I; Supplemental Table S1).

To validate the altered transcript levels of this set of genes in the *mlo2 mlo6 mlo12* triple mutant, we exemplarily compared expression levels of a subset of these by real-time RT-PCR in mature rosette leaves of mutant and wild-type plants. Besides genes that were found at both the top of list A and in list B (*CYP79B2*, *PAD3*, and *WRKY53*), we included *SAG13*, a characteristic marker of early leaf senescence (Lohman et al., 1994), which occurred in list B but was ranked at a lower position in list A (Table I). Consistent with the microarray data, at the late time point (7 weeks) all tested genes showed considerably higher transcript accumulation in the *mlo* triple mutant compared with the wild type (Fig. 3A; Supplemental Fig. S4). In sum, the results of the quantitative RT-PCR analysis corroborate the microarray data, indicating elevated transcript levels of genes of the Trp biosynthesis and metabolism pathways as well as initiation of a senescence-related developmental program in *mlo2 mlo6 mlo12* mutant plants.

We extended the quantitative RT-PCR analysis to investigate whether a similar transcript pattern for the selected genes also occurred in plants grown in long-day conditions. In this experiment, mature rosette leaves were collected at early (4 weeks) and late (5 weeks) time points from plants grown in a pathogen-free environment with a 16-h-light/8-h-dark cycle. The expression patterns of the genes considered were similar to those observed in short-day-grown plants, indicating that the elevated transcript accumulation of these genes in the *mlo2 mlo6 mlo12* triple mutant is independent of short- or long-day growth conditions but dependent on the developmental stage and the genetic background (Fig. 3A).

Comparative Proteomic and Metabolomic Analysis of Wild-Type and *mlo2 mlo6 mlo12* Plants

To study whether the observed changes in the transcriptome would concur with detectable alterations in

Table I. *Selected genes identified by microarray analysis*

Genes related to Trp biosynthesis/metabolism and early leaf senescence were selected by manual inspection of the top of list A (top 150 genes) and list B (Supplemental Table S1).

Arabidopsis Genome Initiative No.	Gene Name	Biochemical Activity of Encoded Protein	Process	Fold Change between Week 7 and Week 5		Rank in List A	Present in List B?
				Col-0	*mlo2 mlo6 mlo12*		
At5g05730	*ASA1*	Synthase	Trp biosynthesis	0.636	1.485	73	No
At2g04400	*IGPS*	Synthase	Trp biosynthesis	0.738	1.5	32	No
At5g17990	*PAT1*	Acyltransferase	Trp biosynthesis	0.577	1.138	78	No
At3g54640	*TSA2*	Synthase	Trp biosynthesis	0.851	3.267	58	Yes
At4g39950	*CYP79B2*	Cytochrome P450	Indole glucosinolate and camalexin biosynthesis	1.389	4.327	117	Yes
At5g57220	*CYP81F2*	Cytochrome P450	Indole glucosinolate biosynthesis	0.416	1.157	12	No
At4g31500	*CYP83B1*	Cytochrome P450	Indole glucosinolate biosynthesis	0.859	1.654	89	No
At1g18570	*MYB51*	Transcriptional regulator	Indole glucosinolate biosynthesis	0.668	2.28	13	No
At1g74100	*SOT16*	Sulfotransferase	Indole glucosinolate biosynthesis	0.704	1.593	22	No
At1g24100	*UGT74B1*	UDP-glucosyltransferase	Indole glucosinolate biosynthesis	0.488	1.123	76	No
At2g30770	*CYP71A13*	Cytochrome P450	Camalexin biosynthesis	0.964	3.679	34	Yes
At3g26830	*CYP71B15* (*PAD3*)	Cytochrome P450	Camalexin biosynthesis	0.797	6.239	3	Yes
At2g29350	*SAG13*	Oxidoreductase	Leaf senescence	1.717	3.759	1,468	Yes
At4g23810	*WRKY53*	Transcriptional regulator	Leaf senescence	0.914	4.902	7	Yes

the leaf proteome, we performed comparative two-dimensional gel electrophoresis of total soluble protein extracts obtained from rosette leaves of 7-week-old plants grown under short-day conditions. This analysis revealed no obvious differences between the *mlo2 mlo6 mlo12* triple mutant and the Col-0 wild type, demonstrating that at this level of resolution deregulated leaf senescence does not correlate with altered protein steady-state levels (Supplemental Fig. S5).

Finally, we conducted a comparative metabolite profile of the *mlo2 mlo6 mlo12* mutant and wild-type plants. Guided by the results of the microarray analysis, we focused this approach on indolic metabolites. Leaf material (leaf 7) was collected from plants grown in short-day conditions at 5, 6, 7, and 8 weeks after sowing. Crude leaf extracts were analyzed by HPLC coupled to a diode array detector or a fluorescence detector. Consistent with the elevated *PAD3* transcript levels (see above), we found a trend toward higher camalexin concentrations in the triple mutant than in the wild type from 6 weeks after sowing onward (Fig. 3B). Similarly, an unknown derivative of camalexin was found at higher levels in the triple mutant at all time points tested (statistically significant at 8 weeks; Supplemental Fig. S6A). A differential pattern similar to the one observed for camalexin and its derivative was also detected for another Trp-derived compound, indol-3-yl-methylamine (I3A; statistically significant at 7 and 8 weeks), which was recently found to be an indole glucosinolate metabolism product that is indirectly linked to plant defense responses (Bednarek et al., 2009). Unlike I3A, two indole glucosinolates, indol-3-yl-methyl glucosinolate (I3G) and its 4-methoxylated derivative 4-methoxy-indol-3-yl-methyl glucosinolate (4MI3G), had lower levels in the triple mutant compared with the wild type (statistically significant at 5, 6, and 8 weeks [I3G] and 6 and 8 weeks [4MI3G]). Taken together, these results indicate that a globally altered profile of Trp-derived metabolites precedes deregulated leaf senescence in the *mlo* triple mutant, raising the possibility that perturbed levels of indolics could be responsible for the latter phenotype.

To find out to what extent the developmentally controlled hyperaccumulation of the Trp-derived metabolites camalexin and I3A is different in the *mlo2 mlo6 mlo12* triple mutant and the *mlo2* single mutant, we examined leaves of 7-week-old plants of these mutant genotypes and of Col-0 wild type. This analysis revealed similar trends but higher absolute levels in the triple mutant than in the *mlo2* single mutant for both metabolites (Fig. 4A). This finding is reminiscent of the quantitative differences in powdery mildew resistance and premature leaf senescence in these two genotypes (Consonni et al., 2006; Fig. 1C) and opens up the possibility to dissect the genetic requirements for the altered accumulation of indolic compounds in the more genetically tractable *mlo2* single mutant.

Trp-Derived Compounds Hyperaccumulating in the *mlo2* Mutant Originate from the Conventional Biosynthetic Route

To examine the contribution of known biosynthetic enzymes to the altered levels of indolics in the *mlo2* mutant, we generated the *mlo2 pad3* double mutant and the *mlo2 cyp79B2 cyp79B3* triple mutant. The *pad3* single mutant and *mlo2 pad3* double mutant revealed quantities of camalexin and its derivative that were close to the detection limit, whereas I3A, I3G, and 4MI3G levels were variable but similar overall to Col-0 wild-type plants and the *mlo2* single mutant (Fig. 4A;

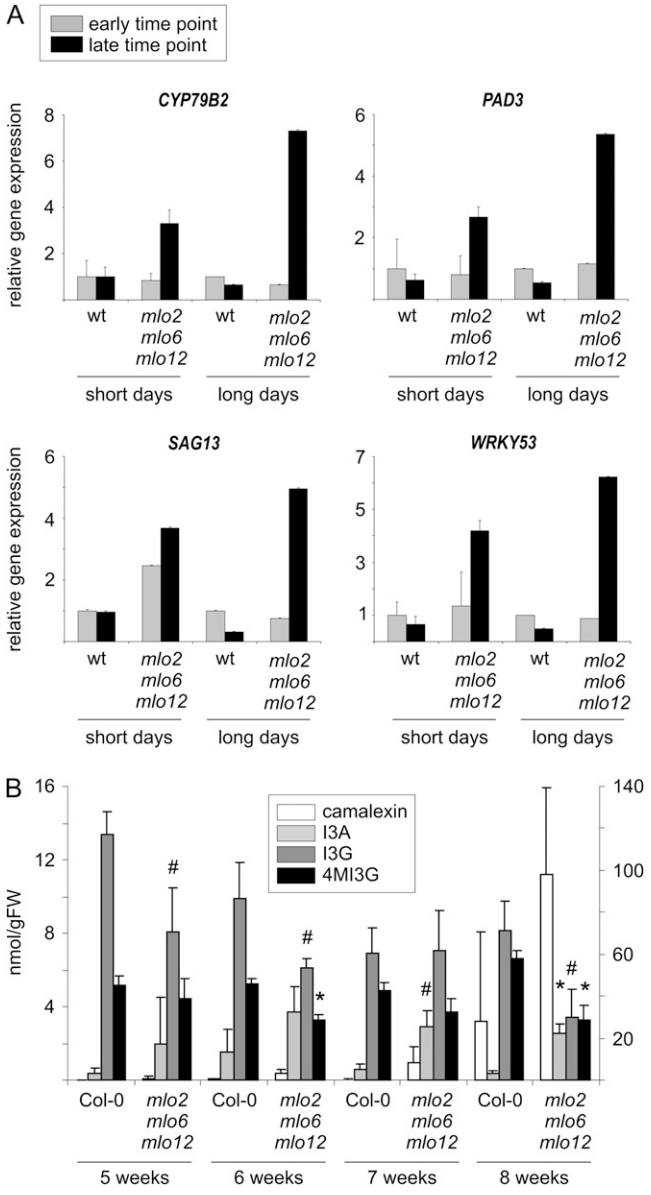

Figure 3. Altered gene expression levels and secondary metabolite accumulation in the Arabidopsis *mlo2 mlo6 mlo12* mutant. A, Expression patterns of genes involved in secondary metabolite biosynthesis and of senescence-associated genes are altered in the *mlo2 mlo6 mlo12* mutant compared with the Col-0 wild type (wt). Gene expression levels determined by quantitative RT-PCR are each presented relative to the expression level in the wild type at the early time point. Values shown represent means ± SD of a representative experiment comprising at least three technical replicates per genotype and time point. Leaf samples of plants grown in short-day conditions were collected at 5 weeks (early time point) and 7 weeks (late time point) after sowing; leaf samples of plants grown in long-day conditions were collected at 4 weeks (early time point) and 5 weeks (late time point) after sowing. Light gray bars show early time point; dark gray bars show late time point. Similar results were obtained in an independent biological experiment (Supplemental Fig. S3). B, Secondary metabolite profile of leaves of the *mlo2 mlo6 mlo12* triple mutant compared with the Col-0 wild type. Rosette leaf 7 of independent plants grown in short-day conditions was collected at 5, 6, 7, and 8 weeks after sowing and used for metabolite analysis. The graphs show the average ± SD of a representative experiment comprising three leaf samples. The experiment was repeated once with similar results. The left *y* axis refers to camalexin and I3A, whereas the right *y* axis applies to I3G and 4MI3G. A statistically significant difference from Col-0 is indicated either by an asterisk ($P < 0.01$; Student's *t* test) or the number sign ($P < 0.05$; Student's *t* test). FW, Fresh weight.

Supplemental Fig. S6B). As expected, the *mlo2 cyp79B2 cyp79B3* triple mutant exhibited undetectable levels of all compounds considered (Fig. 4A; Supplemental Fig. S6B). These results demonstrate that the Trp-derived compounds hyperaccumulating in the *mlo2* mutant originate from their conventional biosynthetic route and that the respective double and triple mutants can be used to assess the role of indolic compounds in *mlo2*-associated premature leaf senescence.

It was recently shown that PEN2 acts as a myrosinase that hydrolyzes both nonsubstituted and 4-methoxylated indole glucosinolates and that is essential for the pathogen-inducible accumulation of the glucosinolate hydrolysis product, I3A (Bednarek et al., 2009). To test whether the *mlo2*-associated increase in levels of this compound is also dependent on PEN2 activity, the *mlo2 pen2* double mutant was analyzed. This double mutant indeed exhibited levels of I3A comparable to the *pen2* single mutant (Fig. 4A), demonstrating the requirement of PEN2 activity for the *mlo2*-mediated I3A hyperaccumulation.

We also examined whether a mutation in the well-characterized senescence-related gene *WRKY53*, which was found to have elevated transcript levels in the *mlo2 mlo6 mlo12* triple mutant (Fig. 2A), was sufficient to restore wild-type levels of Trp derivatives in a *mlo2* genetic background. Therefore, we generated a *mlo2 wrky53* double mutant and performed metabolic profiling. This revealed *mlo2*-like metabolite levels, suggesting that the perturbation of indolic compounds in the *mlo2* mutant is unlikely to be a direct or an indirect consequence of altered *WRKY53* transcript accumulation (Fig. 4A). However, resolution of this analysis is limited, since the differences in indolic metabolite levels between the wild type and the *mlo2* mutant were not statistically significant.

mlo2-Associated Early Leaf Senescence Can Be Uncoupled from the Accumulation of Indolic Metabolites

To determine the role of Trp-derived compounds in *mlo2*-associated early leaf senescence, both whole plant and dark-induced senescence phenotypes were analyzed for the set of mutants described above. No obvious differences were observed between *mlo2* single and *mlo2 pad3* double mutants, whereas a slight enhancement of leaf senescence symptoms was found in the *mlo2 cyp79B2 cyp79B3* triple mutant (Fig. 4B). Notably, a mutation in the gene encoding the senescence regulator WRKY53 did not suppress *mlo2*-associated leaf chlorosis and necrosis (Fig. 4B), indicating that

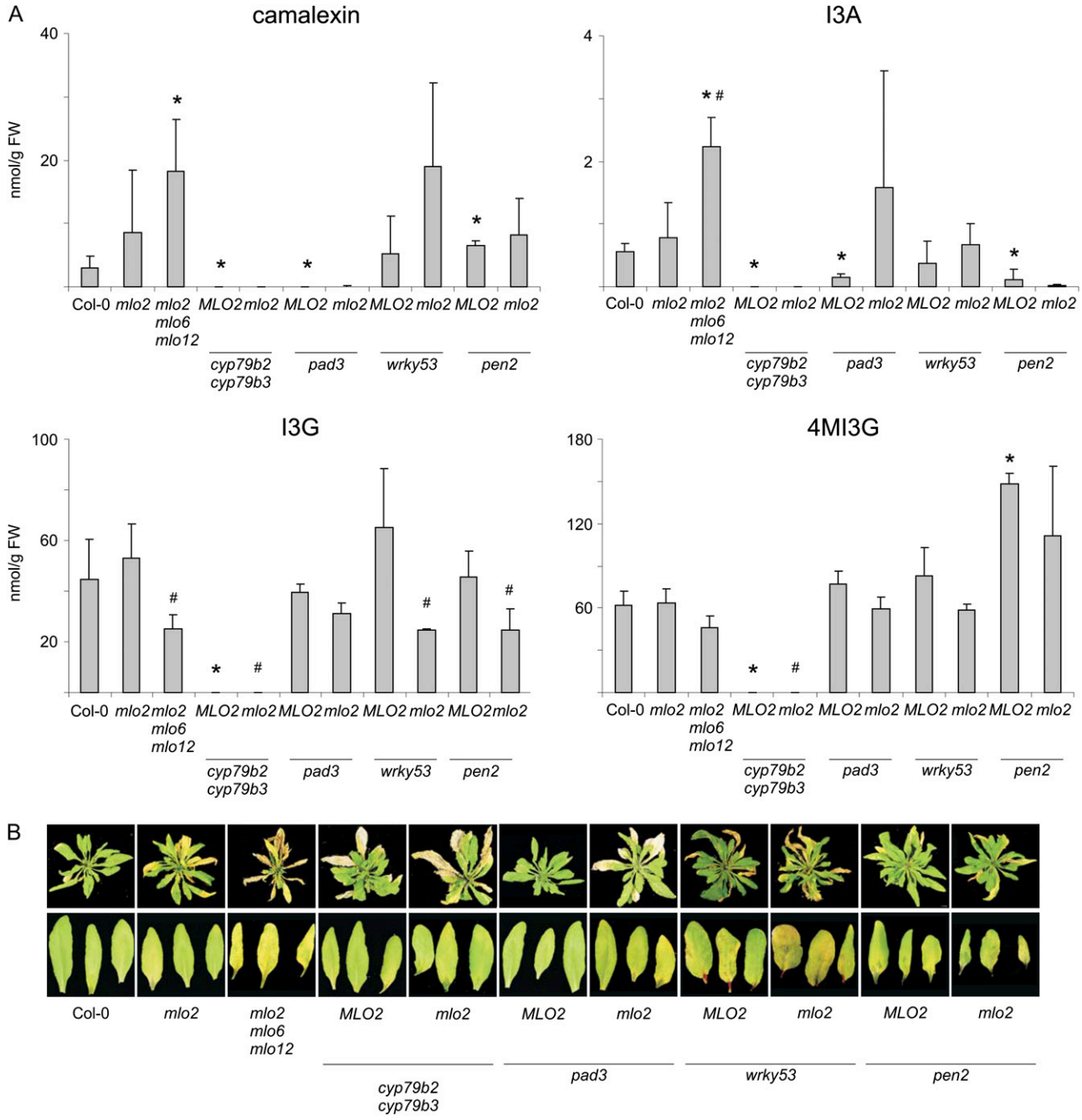

Figure 4. Altered levels of indolic metabolite in leaves of *mlo* mutant plants depend on the conventional biosynthetic route and are not the primary cause of the early leaf senescence phenotype. A, Leaf 7 from nine independent plants grown in short-day conditions was collected at 7 weeks after sowing, and HPLC analysis was performed on metabolite extracts. The graphs show averages ± SD of a representative experiment comprising three technical replicates. One typical experiment out of three is shown. Asterisks denote statistically significant differences ($P < 0.05$; Student's *t* test) from the Col-0 wild type, and number signs denote statistically significant differences ($P < 0.05$; Student's *t* test) from the *mlo2* mutant. FW, Fresh weight. B, Habitus of representative unchallenged (pathogen-free) plants at 7 weeks after sowing (top row) and macroscopic phenotypes of detached leaf 5 from 4-week-old plants dark treated for 4 d (bottom row). Plants were grown in long-day conditions. The experiment was repeated once (except for Col-0, *mlo2*, and *mlo2 mlo6 mlo12*, which had five replicates) with similar results.

the pathway leading to *mlo2*-conditioned premature senescence is either not under the control of WRKY53 or that redundancy in gene functions masks the contribution of this transcriptional regulator in the context of *mlo2*. Early leaf senescence of *mlo2* mutants thus differs at least in this respect from conventional leaf

senescence (Hinderhofer and Zentgraf, 2001). Taken together, these data suggest that altered levels of Trp-derived metabolites and/or aberrant WRKY53 activity are not the major cause of *mlo2*-associated early senescence.

mlo2-Mediated Pathogen Resistance Depends on the Biosynthesis of Indolic Secondary Metabolites

Given the key role of indolic metabolites in defense against nonadapted powdery mildew fungi (Bednarek et al., 2009), we next investigated the functional contribution of Trp-derived compounds in *mlo2*-mediated powdery mildew resistance. We challenged the *mlo2 pad3* double mutant and the *mlo2 cyp79B2 cyp79B3* triple mutant with the adapted pathogen *G. orontii* and quantified infection success by microscopic analysis of fungal host cell entry and conidiophore production (Consonni et al., 2006). The *mlo2 pad3* double mutant displayed partially restored host cell entry and conidiation compared with the *mlo2* single mutant, suggesting a requirement for camalexin for full *mlo2* resistance. Remarkably, the triple mutant *mlo2 cyp79B2 cyp79B3* exhibited an infection phenotype that was similar to the Col-0 wild type, indicating that both camalexin and other indolic metabolites are major determinants of *mlo2* resistance against the adapted powdery mildew pathogen (Fig. 5, A and B). With respect to host cell entry, similar results were also obtained with the nonadapted pea (*Pisum sativum*) powdery mildew pathogen *Erysiphe pisi* (Fig. 5C). However, this plant-pathogen constellation in addition reveals the effect of the *cyp79B2 cyp79B3* double mutant in the context of *MLO2*, which owing to saturating fungal entry levels is masked upon challenge with the adapted powdery mildew pathogen *G. orontii* (Fig. 5, compare B and C). In sum, these data indicate that Trp-derived compounds, including camalexin, are crucial for preinvasion and postinvasion resistance against both adapted and nonadapted powdery mildew fungi in wild-type plants as well as in *mlo2* mutant plants.

The phytoalexin camalexin is known to contribute to defense against necrotrophic fungi (Glazebrook, 2005). It was recently shown that sensitivity of *Botrytis cinerea* to camalexin is isolate specific and that this necrotrophic fungus also exhibits variable sensitivity to indolic glucosinolates (Kliebenstein et al., 2005). We inoculated 4-week-old wild-type and mutant plants with a camalexin-sensitive isolate of *B. cinerea*. Compared with the susceptible Col-0 wild type, the *mlo2* single mutant and *mlo2 mlo6 mlo12* triple mutant were highly resistant, as no spreading lesions were detected upon pathogen treatment (Fig. 6). To test whether this phenotype was also dependent on indolic metabolites, the double mutant *mlo2 pad3* and the triple mutant *mlo2 cyp79B2 cyp79B3* were inoculated with the same *B. cinerea* isolate. Consistent with the effect of these mutations in a wild-type background on camalexin-sensitive *B. cinerea* strains (Kliebenstein et al., 2005), mutations in these genes fully reverted *mlo2*-conditioned resistance (Fig. 6), suggesting that Trp-derived compounds play a major role in *mlo2*-mediated resistance against both biotrophic and necrotrophic fungi.

mlo2 Resistance Is Independent of PMR4/GSL5-Mediated Callose Deposition

mlo2 mutants spontaneously accumulate callose depositions during later developmental stages, before the onset of macroscopically visible signs of early leaf senescence (Consonni et al., 2006). We reasoned that the PMR4/GSL5 callose synthase, which mediates wound and papillary callose deposition in Arabidopsis rosette leaves (Jacobs et al., 2003; Nishimura et al., 2003), could be responsible for this phenotype. To test this hypothesis, the *mlo2 pmr4* double mutant was generated and spontaneous callose deposition was analyzed in a time-course experiment using plants that were not challenged by any pathogen. Lack of the *mlo2*-characteristic callose deposits in rosette leaves of 6-week-old *mlo2 pmr4* double mutant plants demonstrates that the PMR4 glucan synthase-like polypeptide is accountable for the developmentally controlled biosynthesis of callose in *mlo2* (Fig. 7A).

pmr4 plants are macroscopically resistant against powdery mildew attack (Jacobs et al., 2003; Nishimura et al., 2003). In these studies, however, it was not quantitatively resolved at which stage of fungal pathogenesis that resistance in the *pmr4* mutant becomes effective. We challenged control and *pmr4* mutant plants with *G. orontii* and microscopically scored host cell entry and conidiophore formation. This revealed a fungal host cell entry rate in the *pmr4* mutant that is comparable to wild-type plants. In contrast, further development of fungal colonies was found to be severely impaired, resulting in a significant reduction of conidiophore formation (Fig. 7B). A defense response that becomes effective at the postpenetration stage is thus the primary reason for the macroscopic resistance phenotype of the *pmr4* mutant. To investigate whether local pathogen-triggered PMR4-dependent callose deposition in cell wall appositions is required for the *mlo2*-conditioned powdery mildew resistance, the *mlo2 pmr4* double mutant was assessed upon *G. orontii* challenge. Intriguingly, no differences between *mlo2* single and *mlo2 pmr4* double mutant plants were observed with respect to both penetration rate and the level of conidiophore formation (Fig. 7B). This finding indicates that *mlo2* resistance is fully independent of PMR4-mediated callose deposition.

pmr4 mutants were described to constitutively hyperaccumulate SA, and mutations in components of the SA pathway, such as *npr1* and *pad4*, as well as expression of the bacterial salicylate hydroxylase gene, *NahG*, were reported to suppress resistance of *pmr4* mutants against *G. cichoracearum* (Nishimura et al., 2003). To investigate whether powdery mildew resis-

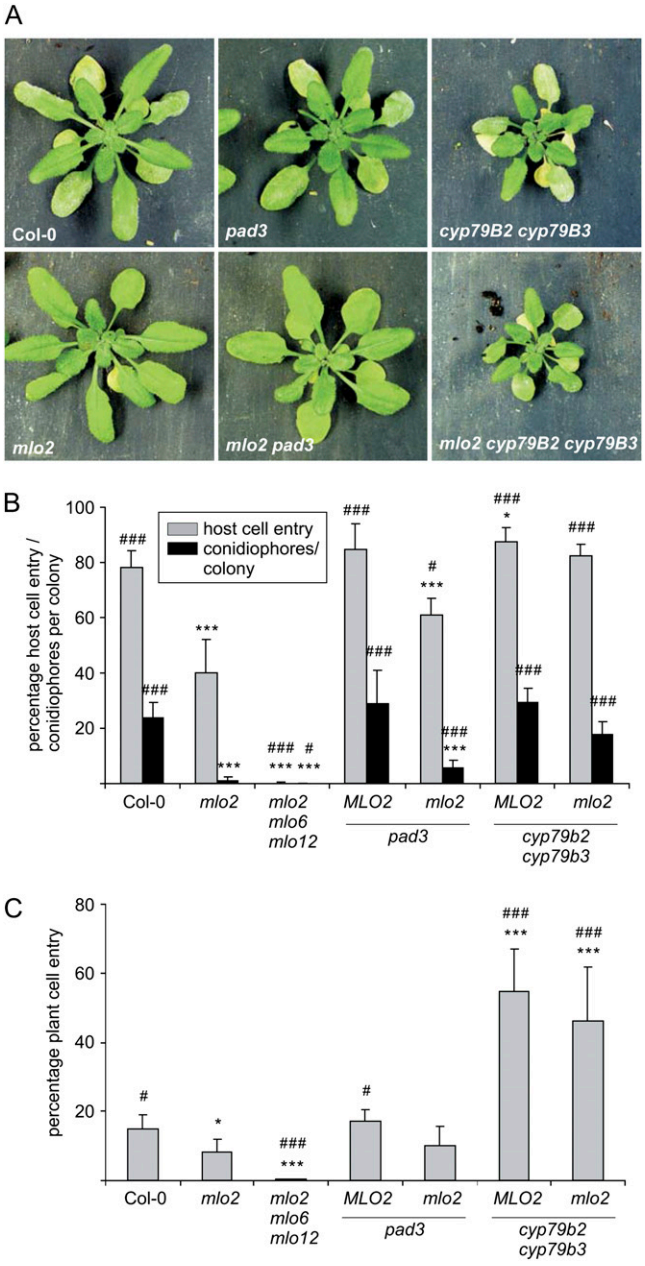

Figure 5. Indolic secondary metabolites are essential for *mlo2*-mediated powdery mildew resistance. A, Representative photographs depicting macroscopic infection phenotypes of wild-type and mutant plants upon challenge with *G. orontii*. Images were taken at 10 d postinoculation. B, Quantitative analysis of *G. orontii* host cell entry (determined at 48 h postinoculation; gray bars) and conidiophore formation (determined at 7 d postinoculation; black bars). Results represent means ± SD of four to eight independent experiments per genotype. Statistically significant differences from the Col-0 wild type are indicated by asterisks (*** $P < 0.01$, * $P < 0.05$; Student's *t* test), and statistically significant differences from *mlo2* are indicated by number signs ($^{###}P < 0.01$, $^{#}P < 0.05$; Student's *t* test). C, Quantitative analysis of *E. pisi* entry into Arabidopsis epidermal cells determined at 7 d postinoculation. Results represent means ± SD of three to six samples per genotype derived from at least three independent experiments. Statistically significant differences from the Col-0 wild type are indicated by asterisks (*** $P < 0.01$, * $P < 0.05$; Student's *t* test), and statistically significant differences from *mlo2* are indicated by number signs ($^{###}P < 0.01$, $^{#}P < 0.05$; Student's *t* test).

tance retained in the *mlo2 pmr4* double mutant was the result of *pmr4*-dependent SA hyperaccumulation, *mlo2 pmr4* plants were crossed with the *sid2* mutant, which is defective in defense-associated SA biosynthesis (Wildermuth et al., 2001), to generate a *mlo2 pmr4 sid2* triple mutant. Both macroscopic and quantitative microscopic analyses of *mlo2 pmr4 sid2* plants challenged with the adapted *G. orontii* revealed a *mlo2*-like phenotype, demonstrating that the resistance retained in the *mlo2 pmr4* double mutant is independent of SA accumulation (Fig. 7B).

Since callose deposition strictly precedes macroscopically visible signs of early leaf senescence in the *mlo2* mutant (Consonni et al., 2006; Supplemental Fig. S7), we reasoned that a causal relationship may dictate the sequential order of the two events. If true, then a genetic block in callose deposition should alleviate the early leaf senescence phenotype of *mlo2* plants. We first assessed the *pmr4* mutant with respect to natural and dark-induced leaf senescence and observed early leaf chlorosis and necrosis that is reminiscent of the *mlo2* mutant phenotype (Fig. 7C). This phenomenon was exaggerated in the *mlo2 pmr4* double mutant, suggesting that the phenotypes of the *mlo2* and *pmr4* mutants are additive and excluding a direct causal link between callose deposition and *mlo2*-conditioned early leaf senescence. To test whether the exaggerated phenotype of the *mlo2 pmr4* double mutant is an effect of the combined SA hyperaccumulation that is known to take place in *mlo2* as well as *pmr4* mutant plants (Nishimura et al., 2003; Consonni et al., 2006), we analyzed whole rosette and dark-induced senescence of the *mlo2 pmr4 sid2* triple mutant. Indeed, lack of *SID2* function partially suppressed both types of senescence in the *mlo2 pmr4* double mutant, suggesting that SA (hyper)accumulation is in part the cause for this phenotype (Fig. 7C).

DISCUSSION

mlo2-Mediated Powdery Mildew Resistance Requires Trp-Derived Secondary Metabolites

In this study, we found that *mlo2* single and *mlo2 mlo6 mlo12* triple mutants accumulate aberrant levels of a subset of Trp-derived compounds during vegetative development (Figs. 3B and 4A). The consistently lower glucosinolate (I3G) but higher glucosinolate breakdown product (I3A) levels in the *mlo2 mlo6 mlo12* mutant compared with wild-type plants point to enhanced glucosinolate turnover being one of the defects in the *mlo* triple mutant (Figs. 3B and 4A). A perturbed profile of indolic metabolites was also recently detected in systemic leaves of the *aux1* mutant,

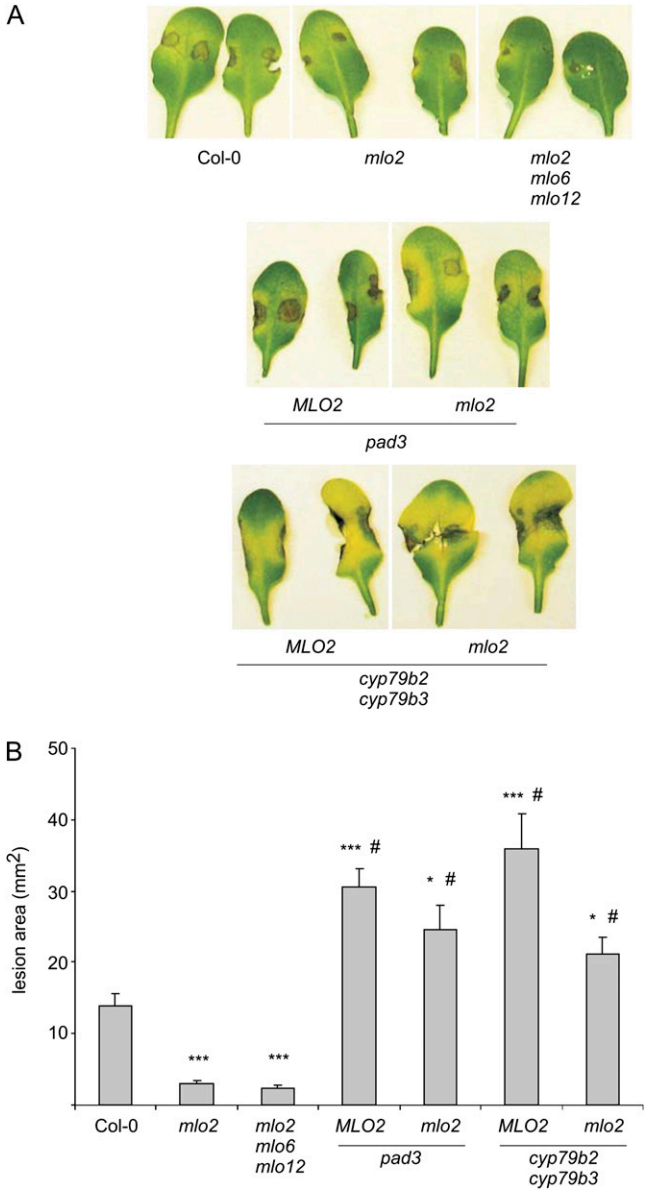

Figure 6. Camalexin is essential for *mlo2*-mediated resistance against *B. cinerea*. A, Representative photographs depicting macroscopic infection phenotypes on leaves of wild-type and mutant plants upon challenge with a camalexin-sensitive strain of *B. cinerea*. Detached leaves of 4-week-old plants grown in 16-h-light/8-h-dark cycles (low light intensity and humidity) were inoculated with two 5-μL droplets of a suspension containing 5×10^5 spores mL^{-1}. Images were taken at 2 d postinoculation. The experiment was repeated twice with similar results. B, Quantitative assessment of lesion diameter determined at 2 d postinoculation with *B. cinerea*. Results originate from one experiment and represent means ± SD of at least nine lesions per genotype. Statistically significant differences from the Col-0 wild type are indicated by asterisks (*** $P < 0.01$, * $P < 0.05$; Student's *t* test), and statistically significant differences from *mlo2* are indicated by number signs ($P < 0.01$; Student's *t* test). The experiment was repeated twice with similar results.

which is defective in the auxin influx transporter AUX1, during the establishment of systemic acquired resistance (Truman et al., 2010).

Among plant secondary metabolites, few indole derivatives have been functionally associated with biotic stress responses. These include the indolic glucosinolates, a class of metabolites restricted to the Brassicales that has been implicated in combating insects (for review, see Halkier and Gershenzon, 2006). Additionally, in Arabidopsis, the phytoalexin camalexin was shown to contribute to resistance against necrotrophic fungi, such as *Alternaria brassicicola* and *B. cinerea* (Thomma et al., 1999b; Ferrari et al., 2003; for review, see Glazebrook, 2005). In contrast, the biotrophic fungus *G. orontii* was reported to be insensitive to camalexin (Reuber et al., 1998). Recently, however, glucosinolate breakdown products with presumptive antimicrobial activity were found to be required for penetration resistance against nonadapted powdery mildew fungi in Arabidopsis, suggesting that at least some indolic compounds contribute to defense against a subset of biotrophic pathogens (Bednarek et al., 2009). In addition to their presumptive direct antimicrobial activity, these metabolites may also have a signaling role in plant innate immunity (Clay et al., 2009). To investigate the contribution of Trp-derived molecules in *mlo2*-associated phenotypes in detail, we generated and analyzed an informative set of Trp metabolism mutants in combination with the *mlo2* single mutant.

We reasoned that altered accumulation patterns of indolic compounds that become apparent during vegetative development (Figs. 3 and 4) might also contribute to the powdery mildew resistance of the *mlo2* mutant. Experimental support for this hypothesis comes from the partially and fully restored susceptibility (host cell entry and conidiation) to *G. orontii* in the *mlo2 pad3* and *mlo2 cyp79B2 cyp79B3* mutants, respectively (Fig. 5, A and B). Furthermore, mutations in *PAD3* or *CYP79B2/CYP79B3* resulted in moderately (*pad3*) or substantially (*cyp79B2 cyp79B3*) increased penetration rates of the nonadapted powdery mildew pathogen *E. pisi*, both in the presence and absence of *MLO2* (Fig. 5C). These findings demonstrate that indolic metabolites, including camalexin, contribute to both preinvasive and postinvasive defense against adapted as well as nonadapted powdery mildew fungi in Arabidopsis. Notably, genetic analyses in the context of systemic acquired resistance indicated that *CYP79B2/CYP79B3* are also required for the establishment of this type of plant immunity, suggesting that indolic metabolites (and possibly the indole-derived phytohormone auxin) contribute either to long-distance signaling or the execution of systemic immune responses (Truman et al., 2010).

This broad indole-mediated antifungal capacity is seemingly masked by the high pathogen success rate in compatible powdery mildew interactions, possibly as a consequence of the ability of adapted pathogens to detoxify these compounds or to suppress pathways that lead to their accumulation. This would explain why the *cyp79B2 cyp79B3* mutant exhibits only a

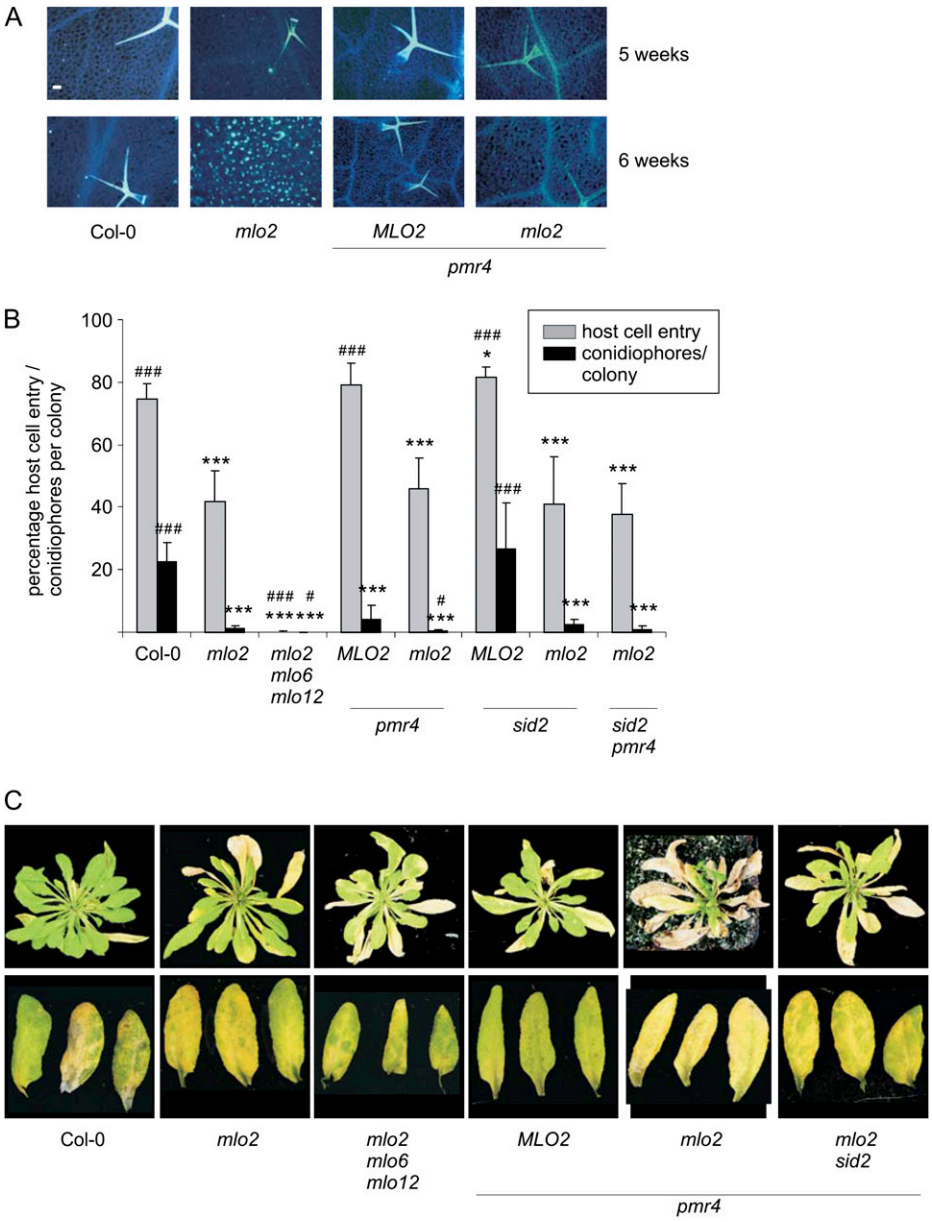

Figure 7. The GSL5/PMR4 callose synthase is required for spontaneous callose deposition but dispensable for penetration resistance of the *mlo2* mutant. A, Representative micrographs of spontaneous callose deposition in unchallenged (pathogen-free) plants grown in long-day conditions. Leaves were collected at the time points indicated. The experiment was repeated once and additionally performed once with plants grown in short-day conditions, yielding similar results. Bar = 50 μm. B, Quantitative analysis of *G. orontii* host cell entry (determined at 48 h postinoculation; gray bars) and conidiophore formation (determined at 7 d postinoculation; black bars). Results represent means ± SD of three to eight independent experiments per genotype. Statistically significant differences from the Col-0 wild type are indicated by asterisks (*** $P < 0.01$, * $P < 0.05$; Student's *t* test), and statistically significant differences from *mlo2* are indicated by number signs ($^{###}$ $P < 0.01$, $^{#}$ $P < 0.05$; Student's *t* test). C, Habitus of representative unchallenged (pathogen-free) plants at 7 weeks after sowing (top row) and macroscopic phenotypes of detached leaf 5 from 4-week-old plants dark-treated for 4 d (bottom row). In both experiments, plants were grown in long-day conditions. The experiment was repeated twice with similar results.

subtle, if any, effect on colonization by the adapted powdery mildew pathogen *G. orontii* (Fig. 5, A and B), while it causes a dramatic increase in plant cell entry by the nonadapted pea powdery mildew pathogen (Fig. 5C). The indolic toxic compounds that, besides camalexin, contribute to defense against powdery mildews currently remain elusive. Metabolomic analyses in the context of powdery mildew-nonhost interactions suggest that a conversion product of 4-methoxylated indole glucosinolate could be the major toxic principle (Bednarek et al., 2009).

It is remarkable that resistance in the *mlo2* mutant is already effective in young plants (5 weeks or younger), before considerable differences in the accumulation of indolic metabolites and the abundance of transcripts that encode for the respective biosynthetic enzymes become evident (Supplemental Fig. S7). One possibility is that substantial cell type-specific differences that may exist between young wild-type and *mlo2* seedlings are diluted in whole leaf-based transcriptomic and metabolomic analyses. Alternatively, despite similar steady-state levels in unchallenged plants, metabolic pathways leading to indolic compounds might be more rapidly activated in *mlo2* mutant plants upon challenge with powdery mildew fungi.

Camalexin Is Required for *mlo2*-Mediated Resistance to *B. cinerea*

Among plant pathogens with a necrotrophic lifestyle, *B. cinerea* is one of the best studied. In Arabidopsis, the well-characterized JA- and ET-dependent

defense signaling pathways have been shown to contribute to basal resistance against *B. cinerea*, since mutants in these pathways showed increased susceptibility to this pathogen (Thomma et al., 1998, 1999a; Ferrari et al., 2003). Additionally, the Arabidopsis-specific phytoalexin camalexin contributes to resistance against *B. cinerea*, as indicated by the increased susceptibility of camalexin-deficient mutants (Ferrari et al., 2003; Kliebenstein et al., 2005; van Baarlen et al., 2007). However, not all isolates of *B. cinerea* are camalexin sensitive (Thomma et al., 1999b; Ferrari et al., 2003); different strains vary in their camalexin tolerance, and this difference determines the ability of the fungal pathogen to proliferate and produce lesions on camalexin-deficient mutants (Kliebenstein et al., 2005). Inoculation of Arabidopsis *mlo2* and *mlo2 mlo6 mlo12* mutants with the necrotrophic fungus *B. cinerea* resulted in severely reduced disease symptoms compared with Col-0 wild-type plants (Fig. 6). This finding is of note since it is, to the best of our knowledge, the first report of enhanced resistance of a *mlo* mutant against a pathogen other than powdery mildews (Jørgensen, 1977; Consonni et al., 2006). Rather conversely, it was previously observed that barley and Arabidopsis *mlo* mutants tend to be more susceptible and/or to show more disease symptoms upon challenge with hemibiotrophic and necrotrophic pathogens, respectively (Jarosch et al., 1999; Kumar et al., 2001; Consonni et al., 2006). The *Botrytis* strain used in our work is camalexin sensitive (Ferrari et al., 2003), suggesting that the increased resistance observed in *mlo* plants might be caused by altered constitutive or pathogen-triggered accumulation patterns of the phytoalexin in these mutants. This hypothesis was supported by the reinstated susceptibility of *mlo2 pad3* and *mlo2 cyp79B2 cyp79B3* double and triple mutants (Fig. 6). Given this finding, it would be interesting to study the infection phenotypes of the Arabidopsis *mlo* mutants upon challenge with a broader range of phytopathogens, preferentially those that are known to be sensitive to camalexin.

mlo2-Associated Leaf Chlorosis/Necrosis Corresponds to a Premature Senescence Program

It has been previously speculated that the developmentally controlled leaf chlorosis and necrosis of barley and Arabidopsis *mlo* mutants corresponds to an authentic senescence process. A comparative time-course analysis performed in the context of a distinct study revealed a premature decay of leaf pigments concomitant with a decline of *glyceraldehyde-3-phosphate dehydrogenase* and an increase in *ubiquitin* transcript accumulation in barley *mlo* mutant plants (Piffanelli et al., 2002). These results suggest that the early leaf cell-death phenotype of barley *mlo* mutants reflects genuine senescence. We expanded this type of analysis to the Arabidopsis *mlo2 mlo6 mlo12* triple mutant and found, in addition to conservation of accelerated chlorophyll catabolism across plant clades, a trend toward an earlier decrease in photochemical efficiency in the mutant plants compared with wild-type plants (Fig. 1, A and B). Moreover, we observed a genotype-specific resemblance of whole plant leaf chlorosis phenotypes upon induction of synchronized artificial (dark-induced) senescence in detached leaves (Fig. 1C). Taken together, these findings strongly suggest that the early leaf chlorosis in barley and Arabidopsis *mlo* mutant plants reflects the premature initiation and possibly accelerated progression of an authentic leaf senescence program. This senescence program might be based on perturbed autophagic processes, since autophagy-deficient mutants *atg2* and *atg5* resemble the SA-dependent early leaf chlorosis/necrosis phenotype of *mlo* mutants (Yoshimoto et al., 2009).

We further investigated the effect of premature leaf senescence in the *mlo2 mlo6 mlo12* mutant at both the transcriptional and proteomic levels. Among the differentially expressed genes are *WRKY53* and *SAG13*, two marker genes of early leaf senescence. WRKY53 is a transcriptional regulator with a well-established role in the control of leaf senescence; mutants in *WRKY53* show delayed onset of senescence, while *WRKY53* overexpression results in early senescence (Hinderhofer and Zentgraf, 2001; Miao et al., 2004). Genetic epistasis analysis suggests that hyperaccumulation of *WRKY53* transcripts in the *mlo2* mutant background is not responsible for *mlo2*-associated leaf senescence (Fig. 3B). Transcription of *WRKY53* is activated by SA (Dong et al., 2003), and the function of WRKY53 in regulating leaf senescence is dependent on the JA/SA equilibrium (Miao and Zentgraf, 2007). Since 7-week-old *mlo2 mlo6 mlo12* mutants were previously shown to possess high levels of SA (Consonni et al., 2006), elevated transcript accumulation of *WRKY53* in the *mlo2 mlo6 mlo12* mu-

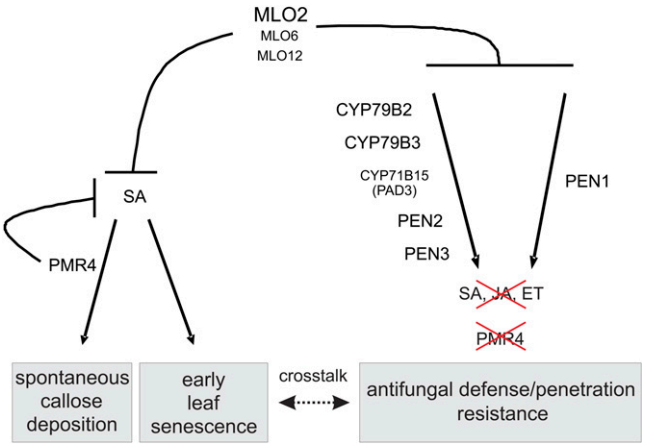

Figure 8. Proposed model for MLO-mediated control of defense to powdery mildew fungi and early leaf senescence/callose deposition. The model integrates previous data (Consonni et al., 2006) and findings of this work. The font size of the components symbolizes the weight of their functional contributions. Components marked by red crosses are not required for a given pathway. [See online article for color version of this figure.]

tant could thus be a consequence of the aberrant SA levels in the triple mutant.

Based on the results of metabolite profiling, we speculated that the developmentally controlled hyperaccumulation of indolic metabolites might drive *mlo* mutants into early leaf senescence. However, even a complete block in the biosynthesis of indolic metabolites (such as in the *mlo2 cyp79B2 cyp79B3* triple mutant) did not reverse the early senescence phenotype of *mlo2* mutants, suggesting that deregulated accumulation of these compounds is not the primary cause for the early senescence phenotype of *mlo2* mutants. It remains a future challenge to further disentangle the molecular events that lead to this *mlo*-associated phenotype.

Callose Biosynthesis Is Not Required for *mlo2* Resistance

Cell wall appositions have long been thought to locally reinforce the cell wall during pathogen attack and were assumed to represent an essential first physical barrier to prevent fungal ingress (Schmelzer, 2002). In this context, callose was for a long time believed to provide a structural reinforcement of papillae (Smart et al., 1986). Nevertheless, recent experiments have questioned the role of callose in plant defense against diverse pathogen classes (Jacobs et al., 2003; Nishimura et al., 2003; Galletti et al., 2008).

Analysis of the *mlo2 pmr4* double mutant revealed that PMR4 activity is required for spontaneous callose deposition in the *mlo2* mutant (Fig. 7A). However, *mlo2*-mediated resistance against *G. orontii* was not affected in this double mutant, suggesting that local callose deposition at attempted fungal entry sites is not obligatory for *mlo2*-mediated penetration resistance against powdery mildews in Arabidopsis (Fig. 7B). The powdery mildew resistance retained in the *mlo2 pmr4* double mutant is not because of a *pmr4*-conditioned hyperactivation of SA-dependent defense reactions, since an additional mutation in the SA biosynthesis gene, *SID2*, likewise resulted in unaffected *mlo2*-like resistance in the *mlo2 pmr4 sid2* triple mutant (Fig. 7B). In sum, these data suggest that, contrary to common belief, callose deposition in papillae is not causative for antifungal penetration resistance.

CONCLUSION

We previously hypothesized that resistance conferred by innate immune pathways and *mlo*-mediated powdery mildew resistance share common defense execution machinery (Humphry et al., 2006). The results obtained in this study substantiate this notion and further highlight the crucial contribution of indolic metabolites in both preinvasive and postinvasive antifungal defense in Arabidopsis. The fact that mutations in *PEN2* restore powdery mildew susceptibility in the *mlo2* mutant to a similar extent as a complete block of biosynthesis of indole-type secondary metabolites (*cyp79B2 cyp79B3* mutant) suggests that PEN2 catalyzes a rate-limiting step in this defense pathway that leads to the major toxic principle(s). The finding that transcripts of the very same genes that are crucial for antifungal defense accumulate during the establishment of early leaf senescence in the *mlo2* mutant provides additional support for the molecular link and potential cross talk between these two processes (Schenk et al., 2005). We propose a model in which MLO proteins negatively regulate both pathways (Fig. 8). Further work is required to unravel how this hypothesized negative regulation is exerted and how the various processes modulated by MLO proteins are interconnected.

MATERIALS AND METHODS

Plant Material and Growth Conditions

Plants were soil grown in controlled-environment chambers under a regime of either a 10-h (short-day) or 16-h (long-day) light period at 150 to 200 μmol m^{-2} s^{-1}, 22°C, and 65% relative humidity, unless otherwise indicated. Arabidopsis (*Arabidopsis thaliana*) wild-type Col-0, *mlo2* (*mlo2-5*), *mlo2 mlo6 mlo12* (*mlo2-5 mlo6-2 mlo12-1*; Consonni et al., 2006), *pad3* (*pad3-1*; Glazebrook and Ausubel, 1994), *cyp79B2 cyp79B3* (Zhao et al., 2002), *wrky53* (Miao et al., 2004), *pen2* (*pen2-1*; Lipka et al., 2005), and *pmr4* (*pmr4-1*; Nishimura et al., 2003) mutants have been previously described. Homozygous double and triple mutants were selected by PCR analysis from intermutant crosses using these lines as parents. Homozygous insertion mutants were identified by PCR using T-DNA- and gene-specific primer sets as described on the T-DNA Express Web site (http://signal.salk.edu/cgi-bin/tdnaexpress). Primer sequences are available on request. The transgenic *MLO2* promoter::*GUS* reporter line has been described before (Chen et al., 2006). Four-week-old plants were used for *Golovinomyces orontii*, *Erysiphe pisi*, and *Botrytis cinerea* inoculation experiments.

Phytopathogens

Powdery mildews used in this study were the isolates of *G. orontii* and *E. pisi* kept at the Max-Planck Institute for Plant Breeding Research (Lipka et al., 2005). The camalexin-sensitive *B. cinerea* strain was originally isolated from *Brassica oleracea* (Ferrari et al., 2003; J. Plotnikova, unpublished results). Inoculation of Arabidopsis with *B. cinerea* was performed as described previously (Ferrari et al., 2003).

Microarray Experiment and Data Analysis

Mature rosette leaves (six per genotype and time point) were harvested at 5, 6, and 7 weeks after sowing. Total RNA was extracted using the Trizol reagent and purified with the RNeasy Plant RNA Purification kit (Qiagen). Copy RNA (cRNA) was prepared following the manufacturer's instructions (www.affymetrix.com/support/technical/manual/expression_manual.affx). Labeled cRNA transcripts were purified using the sample cleanup module (Affymetrix). Fragmentation of cRNA transcripts, hybridization, and scanning of the high-density oligonucleotide microarrays (Arabidopsis ATH1 genome array; Affymetrix) were performed according to the manufacturer's GeneChip Expression Analysis Technical Manual. A single experiment with one microarray per time point and genotype was performed. Quality of the data was evaluated at probe level by examining the arrays for spatial effects, distribution of absent and present calls, and the intensity of spike-in controls. We used the robust multiarray average procedure (Irizarry et al., 2003) to correct for background effects and chip effects and to summarize the probe values into probe set values, resulting in 22,810 normalized expression values per array. The raw and normalized data have been deposited in the Gene Expression Omnibus (http://www.ncbi.nlm.nih.gov/geo) and are accessible through Gene Expression Omnibus record GSE17875. R/Bioconductor (Gentleman et al., 2004) was used to preprocess the raw microarray data.

To identify candidate genes with potentially altered transcript accumulation in the *mlo2 mlo6 mlo12* triple mutant during development, we performed two different computations. In one procedure, we first calculated the ratio of the mean expression values at 6 and 7 weeks to the expression values at week 5 for both the wild type and the mutant. We then calculated the ratio of the respective values for the mutant and the wild type and generated a list ranked by descending ratios based on this result. The produced list (list A) contains all 22,810 genes and provides a full overview of the genes for which the average transcript levels in weeks 6 and 7 increased disproportionately in the triple mutant in comparison with week 5, irrespective of the actual absolute transcript levels. The reported ratios and expression values in list A are on an arithmetic scale, while computations were performed on a logarithmic scale. In the second procedure, we generated a hit list (list B) that represents a fraction of the original gene number (22,810 genes) by subsequently applying the following criteria. First, we selected genes that at 7 weeks showed an at least 2-fold higher transcript accumulation in the mutant than in the wild type (M7 > 2× C7; 326 genes in total). Within these 326 genes, we then selected those that exhibited at least 2-fold microarray values at 7 weeks compared with 5 weeks in the triple mutant (M7 > 2× M5; 181 genes). Next, we selected those for which the increase in transcript levels in the mutant from 5 to 7 weeks was at least 2-fold higher compared with the respective increase in the wild type [(M7/M5) > 2× (C7/C5); 135 genes]. Finally, we eliminated those genes for which all six microarray values were below 40, resulting in a final list with a total of 98 genes. This list (list B) represents genes with elevated transcript levels specific to the mutant at week 7 in comparison with week 5 while ensuring that absolute fold changes and transcript levels are high.

To find differentially regulated pathways, we first obtained predefined sets of genes with the same GO term (http://www.geneontolgy.org) as defined in the ath1121501 annotation library available from R/Bioconductor. We then used a Wilcoxon rank test, as implemented in the function "geneSetTest" of the Limma package (Smyth, 2005), to test whether genes with the same GO term are more highly ranked in list A compared with randomly selected genes. A Fisher's exact test, as implemented in GOstat (Beißbarth and Speed, 2004), was used to test for overrepresented GO terms in the 98 genes of list B. Correction for multiple testing was done in both cases by controlling the false discovery rate (Benjamini and Hochberg, 1995).

RNA Isolation, cDNA Synthesis, and Quantitative RT-PCR

Total RNA was isolated using the Trizol reagent according to the manufacturer's instructions (Invitrogen). The isolated RNA was further purified using RNeasy mini columns (Qiagen) according to the manufacturer's instructions. cDNA was synthesized using SuperScript RTII reverse transcriptase according to the manufacturer's instructions (Invitrogen).

To quantify gene expression using real time RT-PCR, the forward and reverse primers of each gene were as follows: 5′-ACGATCATTTAACCGCTTGG-3′ and 5′-CAAACATTGCTTCCATGTGC-3′ for *CYP79B2* (At4g15110); 5′-ACGAGCATCTTAAGCCTGGA-3′ and 5′-CCCAAGTGTTGTCCGAATCT-3′ for *PAD3* (At3g26830); 5′-CATGACCGCTCTTGTCACTG-3′ and 5′-TCGCAGACAGAAGTGGTGAC-3′ for *SAG13* (At2g29350); 5′-AAACTGTTGGGCAACGAAAC-3′ and 5′-AATGGCTGGTTTGACTCTGG-3′ for *WRKY53* (At4g23810); and 5′-ACTGAGCACAATGTTAC-3′ and 5′-GGTGATGGTGTGTCT-3′ for *Actin2* (At3g18780). *Actin2* was used as an internal control to normalize gene expression across different samples. The reactions were conducted on a 7500 Real-Time PCR system (Applied Biosystems) using SYBR Green (Applied Biosystems) with the following conditions: 95°C for 10 min (1×); 95°C for 15 s and 56.5°C for 1 min (40×); followed by the dissociation curve analysis to verify the presence of a single amplicon in each reaction. The fold change in the target gene, normalized to *Actin2* and relative to the gene expression in the control sample, was calculated according to the comparative cycle threshold (ΔΔct) method as described (Libault et al., 2007).

Protein Extraction and Two-Dimensional PAGE

Total protein extracts from rosette leaves of 7-week-old plants grown in short-day conditions were prepared as described (Noir et al., 2009). Briefly, plant material was ground in liquid nitrogen, and 1 mL of extraction buffer (50 mM Tris, pH 8.0, 10 mM EDTA, 10 mM dithiothreitol, 0.5% CHAPS, and one protease inhibitor cocktail tablet [Roche]) was added. Proteins were extracted by repeated cycles of vortexing and chilling. Cell debris was removed by centrifugation, and the supernatant was subjected to TCA/acetone precipitation. Two-dimensional PAGE and protein staining were performed as described (Noir et al., 2009) except that 100 μg of protein was loaded per gel. SeeBlue Plus2 prestained standard was used for estimating M_r values. False-colored protein pattern overlays were generated using Proteomeweaver two-dimensional analysis software version 4.0 (Bio-Rad).

Extraction of Secondary Metabolites and HPLC Analysis

Rosette leaves (leaf 7) of Col-0 and *mlo2 mlo6 mlo12* triple mutant plants were collected and frozen in liquid nitrogen. After addition of dimethyl sulfoxide (50 μL 20 mg^{-1} fresh weight), the tissue was homogenized using zirconia beads (1 mm; Roth) in a Mini-Beadbeater-8 (Biospec Products) and centrifuged for 15 min at 20,000*g*. The supernatants were collected and subjected to HPLC on an Agilent 1100 HPLC system equipped with diode array detector and fluorescence detector. Samples were analyzed on an Atlantis T3 C18 column (150 mm × 2.1 mm, 3 μm; Waters) using 0.1% trifluoroacetic acid as solvent A and 98% acetonitrile/0.1% trifluoroacetic acid as solvent B at a flow rate of 0.25 mL min^{-1} at 22°C (gradient of solvent A: 100% at 0 min, 100% at 2 min, 90% at 9 min, 72% at 30 min, 50% at 33 min, 20% at 40 min, and 100% at 41 min). Camalexin was analyzed on a Zorbax Extend-C18 column (100 × 2.1 mm, 3.5 μm; Agilent) using water as solvent A and 98% acetonitrile as solvent B at a flow rate of 0.3 mL min^{-1} at 22°C (gradient of solvent A: 96% at 0 min, 96% at 3 min, 70% at 20 min, 20% at 33 min, and 0% at 34 min). The concentrations of the metabolites of interest were quantified based on the comparison of their peak areas with those obtained during HPLC analyses of known amounts of the respective compounds purified from plant tissue (I3G) or synthetic (I3A, camalexin) standards.

Analysis of Chlorophyll Content

Approximately 20 wild-type and mutant plants were grown on soil in long-day conditions. Three independent samples of leaf 7 were taken for each genotype and time point, starting from 28 d after sowing, with intervals ranging from 2 to 6 d. Chlorophyll was isolated from leaf tissue by homogenization in liquid nitrogen and subsequent extraction into 80% (v/v) acetone saturated with KOH. After centrifugation (10 min, 13,000*g*), chlorophyll concentrations were determined spectrophotometrically at 664, 647, and 750 nm (Strain et al., 1971; Pruzinská et al., 2005).

F_v/F_m Measurements

F_v/F_m was measured in vivo using a pulse amplitude modulation 101/103 fluorometer (Walz), starting from 28 d after sowing, at intervals of 2 to 6 d. After 30 min of incubation in the dark, saturating pulses of white light (0.8 s, 6,000 μmol photons m^{-2} s^{-1}) were applied and F_v/F_m was calculated (Varotto et al., 2000; Pesaresi et al., 2002; Oh et al., 2003; Ihnatowicz et al., 2004). Leaf 7 of four independent plants grown in long-day conditions was used per genotype and time point.

Dark-Induced Senescence

Leaf 5 from 4-week-old Arabidopsis plants grown in long-day conditions were excised and placed on moisturized filter paper in petri dishes with the adaxial side facing up. The plates were kept in darkness at 22°C and controlled conditions for 4 d (Pruzinská et al., 2005; Guo and Gan, 2006).

Callose Deposition

For visualization of callose, samples were stained with aniline blue as described (Adam and Somerville, 1996). Data were obtained from two independent experiments with five plants each per genotype and experiment.

Quantification of Fungal Infection Success

For visualization of epiphytic fungal structures, specimens were briefly stained in 0.6% Coomassie Brilliant Blue (in ethanol) and then rinsed with water. Due to the small size of respective haustoria, differentiation of elongating secondary hyphae served as an approximation of penetration success in the powdery mildew species *G. orontii* and *E. pisi*. Data were obtained from

a minimum of three independent experiments with five plants each per genotype and experiment.

Supplemental Data

The following materials are available in the online version of this article.

Supplemental Figure S1. Scheme of the Trp and indole biosynthetic pathway.

Supplemental Figure S2. Independent biological replicate of the analysis of photosynthetic performance and chlorophyll content shown in Figure 1A.

Supplemental Figure S3. Unsupervised hierarchical cluster of the microarray data.

Supplemental Figure S4. Independent biological replicate of the RT-PCR analysis shown in Figure 3A.

Supplemental Figure S5. Two-dimensional gel electrophoresis reveals no differences between the proteomes of wild-type and *mlo2 mlo6 mlo12* mutant plants.

Supplemental Figure S6. Accumulation of an unknown camalexin derivative in wild-type and mutant plants.

Supplemental Figure S7. Timing of events and phenotypes in the *mlo2* or *mlo2 mlo6 mlo12* mutant.

Supplemental Table S1. Genes identified as differentially regulated in the *mlo2 mlo6 mlo12* mutant throughout development.

ACKNOWLEDGMENTS

We thank Anja Reinstädler and Corinna Liller for excellent technical assistance and Ania Ihnatowicz for help with the pulse amplitude modulation measurement. We also acknowledge Dr. Imre Somssich for providing seeds of the *wrky53* mutant.

Received October 27, 2009; accepted December 14, 2009; published December 18, 2009.

LITERATURE CITED

Adam L, Somerville SC (1996) Genetic characterization of five powdery mildew disease resistance loci in *Arabidopsis thaliana*. Plant J **9:** 341–356

Aist JR (1976) Papillae and related wound plugs of plant cells. Annu Rev Phytopathol **14:** 145–163

Bayles CJ, Ghemawat MS, Aist JR (1990) Inhibition by 2-deoxy-D-glucose of callose formation, papilla deposition, and resistance to powdery mildew in an *ml-o* barley mutant. Physiol Mol Plant Pathol **36:** 63–72

Bednarek P, Pislewska-Bednarek M, Svatos A, Schneider B, Doubsky J, Mansurova M, Humphry M, Consonni C, Panstruga R, Sanchez-Vallet A, et al (2009) A glucosinolate metabolism pathway in living plant cells mediates broad-spectrum antifungal defense. Science **323:** 101–106

Beißbarth T, Speed TP (2004) GOstat: find statistically overrepresented Gene Ontologies within a group of genes. Bioinformatics **20:** 1464–1465

Benjamini Y, Hochberg Y (1995) Controlling the false discovery rate: a practical and powerful approach to multiple testing. J R Stat Soc Series B Stat Methodol **57:** 289–300

Boyes DC, Zayed AM, Ascenzi R, McCaskill AJ, Hoffman NE, Davis KR, Gorlach J (2001) Growth stage-based phenotypic analysis of *Arabidopsis*: a model for high throughput functional genomics in plants. Plant Cell **13:** 1499–1510

Büschges R, Hollricher K, Panstruga R, Simons G, Wolter M, Frijters A, van Daelen R, van der Lee T, Diergaarde P, Groenendijk J, et al (1997) The barley *Mlo* gene: a novel control element of plant pathogen resistance. Cell **88:** 695–705

Chen ZY, Hartmann HA, Wu MJ, Friedman EJ, Chen JG, Pulley M, Schulze-Lefert P, Panstruga R, Jones AM (2006) Expression analysis of the *AtMLO* gene family encoding plant-specific seven-transmembrane domain proteins. Plant Mol Biol **60:** 583–597

Clay NK, Adio AM, Denoux C, Jander G, Ausubel FM (2009) Glucosinolate metabolites required for an Arabidopsis innate immune response. Science **323:** 95–101

Collins NC, Thordal-Christensen H, Lipka V, Bau S, Kombrink E, Qiu JL, Hückelhoven R, Stein M, Freialdenhoven A, Somerville SC, et al (2003) SNARE-protein-mediated disease resistance at the plant cell wall. Nature **425:** 973–977

Consonni C, Humphry ME, Hartmann HA, Livaja M, Durner J, Westphal L, Vogel J, Lipka V, Kemmerling B, Schulze-Lefert P, et al (2006) Conserved requirement for a plant host cell protein in powdery mildew pathogenesis. Nat Genet **38:** 716–720

Devoto A, Hartmann HA, Piffanelli P, Elliott C, Simmons C, Taramino G, Goh CS, Cohen FE, Emerson BC, Schulze-Lefert P, et al (2003) Molecular phylogeny and evolution of the plant-specific seven-transmembrane MLO family. J Mol Evol **56:** 77–88

Dong JX, Chen CH, Chen ZX (2003) Expression profiles of the Arabidopsis WRKY gene superfamily during plant defense response. Plant Mol Biol **51:** 21–37

Eichmann R, Hückelhoven R (2008) Accommodation of powdery mildew fungi in intact plant cells. J Plant Physiol **165:** 5–18

Ferrari S, Plotnikova JM, De Lorenzo G, Ausubel FM (2003) Arabidopsis local resistance to *Botrytis cinerea* involves salicylic acid and camalexin and requires EDS4 and PAD2, but not SID2, EDS5 or PAD4. Plant J **35:** 193–205

Galletti R, Denoux C, Gambetta S, Dewdney J, Ausubel FM, De Lorenzo G, Ferrari S (2008) The AtrbohD-mediated oxidative burst elicited by oligogalacturonides in Arabidopsis is dispensable for the activation of defense responses effective against *Botrytis cinerea*. Plant Physiol **148:** 1695–1706

Gentleman RC, Carey VJ, Bates DM, Bolstad B, Dettling M, Dudoit S, Ellis B, Gautier L, Ge YC, Gentry J, et al (2004) Bioconductor: open software development for computational biology and bioinformatics. Genome Biol **5:** R80

Gigolashvili T, Berger B, Mock HP, Muller C, Weisshaar B, Fluegge UI (2007) The transcription factor HIG1/MYB51 regulates indolic glucosinolate biosynthesis in Arabidopsis thaliana. Plant J **50:** 886–901

Glawischnig E (2007) Camalexin. Phytochemistry **68:** 401–406

Glawischnig E, Hansen BG, Olsen CE, Halkier BA (2004) Camalexin is synthesized from indole-3-acetaidoxime, a key branching point between primary and secondary metabolism in Arabidopsis. Proc Natl Acad Sci USA **101:** 8245–8250

Glazebrook J (2005) Contrasting mechanisms of defense against biotrophic and necrotrophic pathogens. Annu Rev Phytopathol **43:** 205–227

Glazebrook J, Ausubel FM (1994) Isolation of phytoalexin-deficient mutants of *Arabidopsis thaliana* and characterization of their interactions with bacterial pathogens. Proc Natl Acad Sci USA **91:** 8955–8959

Guo YF, Gan SS (2006) AtNAP, a NAC family transcription factor, has an important role in leaf senescence. Plant J **46:** 601–612

Halkier BA, Gershenzon J (2006) Biology and biochemistry of glucosinolates. Annu Rev Plant Biol **57:** 303–333

Hinderhofer K, Zentgraf U (2001) Identification of a transcription factor specifically expressed at the onset of leaf senescence. Planta **213:** 469–473

Hull AK, Vij R, Celenza JL (2000) *Arabidopsis* cytochrome P450s that catalyze the first step of tryptophan-dependent indole-3-acetic acid biosynthesis. Proc Natl Acad Sci USA **97:** 2379–2384

Humphry M, Consonni C, Panstruga R (2006) *mlo*-based powdery mildew immunity: silver bullet or simply non-host resistance? Mol Plant Pathol **7:** 605–610

Ihnatowicz A, Pesaresi P, Varotto C, Richly E, Schneider A, Jahns P, Salamini F, Leister D (2004) Mutants for photosystem I subunit D of *Arabidopsis thaliana*: effects on photosynthesis, photosystem I stability and expression of nuclear genes for chloroplast functions. Plant J **37:** 839–852

Irizarry RA, Hobbs B, Collin F, Beazer-Barclay YD, Antonellis KJ, Scherf U, Speed TP (2003) Exploration, normalization, and summaries of high density oligonucleotide array probe level data. Biostatistics **4:** 249–264

Jacobs AK, Lipka V, Burton RA, Panstruga R, Strizhov N, Schulze-Lefert P, Fincher GB (2003) An *Arabidopsis* callose synthase, GSL5, is required for wound and papillary callose formation. Plant Cell **15:** 2503–2513

Jarosch B, Kogel KH, Schaffrath U (1999) The ambivalence of the barley *Mlo* locus: mutations conferring resistance against powdery mildew (*Blumeria graminis* f. sp. *hordei*) enhance susceptibility to the rice blast fungus *Magnaporthe grisea*. Mol Plant Microbe Interact **12:** 508–514

Jørgensen JH (1977) Spectrum of resistance conferred by *ML-O* powdery mildew resistance genes in barley. Euphytica **26:** 55–62

Jørgensen JH (1992) Discovery, characterization and exploitation of Mlo powdery mildew resistance in barley. Euphytica **63:** 141–152

Kim KS, Giacomelii GA, Sase S, Son JE, Nam SW, Nakazawa F (2006) Optimization of growth environment in a plant production facility using a chlorophyll fluorescence method. Jpn Agric Res Q **40:** 149–156

Kliebenstein DJ, Rowe HC, Denby KJ (2005) Secondary metabolites influence Arabidopsis/*Botrytis* interactions: variation in host production and pathogen sensitivity. Plant J **44:** 25–36

Kumar J, Hückelhoven R, Beckhove U, Nagarajan S, Kogel KH (2001) A compromised Mlo pathway affects the response of barley to the necrotrophic fungus *Bipolaris sorokiniana* (Teleomorph : *Cochliobolus sativus*) and its toxins. Phytopathology **91:** 127–133

Kusaba M, Ito H, Morita R, Iida S, Sato Y, Fujimoto M, Kawasaki S, Tanaka R, Hirochika H, Nishimura M, et al (2007) Rice NON-YELLOW COLORING1 is involved in light-harvesting complex II and grana degradation during leaf senescence. Plant Cell **19:** 1362–1375

Kwon C, Neu C, Pajonk S, Yun HS, Lipka U, Humphry M, Bau S, Straus M, Kwaaitaal M, Rampelt H, et al (2008) Co-option of a default secretory pathway for plant immune responses. Nature **451:** 835–840

Libault M, Wan JR, Czechowski T, Udvardi M, Stacey G (2007) Identification of 118 Arabidopsis transcription factor and 30 ubiquitin-ligase genes responding to chitin, a plant-defense elicitor. Mol Plant Microbe Interact **20:** 900–911

Lipka V, Dittgen J, Bednarek P, Bhat R, Wiermer M, Stein M, Landtag J, Brandt W, Rosahl S, Scheel D, et al (2005) Pre- and postinvasion defenses both contribute to nonhost resistance in *Arabidopsis*. Science **310:** 1180–1183

Lohman KN, Gan S, John MC, Amasino RM (1994) Molecular analysis of natural leaf senescence in *Arabidopsis thaliana*. Physiol Plant **92:** 322–328

Maxwell K, Johnson GN (2000) Chlorophyll fluorescence: a practical guide. J Exp Bot **51:** 659–668

Miao Y, Laun T, Zimmermann P, Zentgraf U (2004) Targets of the WRKY53 transcription factor and its role during leaf senescence in Arabidopsis. Plant Mol Biol **55:** 853–867

Miao Y, Zentgraf U (2007) The antagonist function of *Arabidopsis* WRKY53 and ESR/ESP in leaf senescence is modulated by the jasmonic and salicylic acid equilibrium. Plant Cell **19:** 819–830

Micali C, Göllner K, Humphry M, Consonni C, Panstruga R (2008) The powdery mildew disease of Arabidopsis: a paradigm for the interaction between plants and biotrophic fungi. *In* The Arabidopsis Book. American Society of Plant Biologists, Rockville, MD, doi/10.1199/tab.0115, http://www.aspb.org/publications/arabidopsis/

Mikkelsen MD, Hansen CH, Wittstock U, Halkier BA (2000) Cytochrome P450CYP79B2 from *Arabidopsis* catalyzes the conversion of tryptophan to indole-3-acetaldoxime, a precursor of indole glucosinolates and indole-3-acetic acid. J Biol Chem **275:** 33712–33717

Nishimura MT, Stein M, Hou BH, Vogel JP, Edwards H, Somerville SC (2003) Loss of a callose synthase results in salicylic acid-dependent disease resistance. Science **301:** 969–972

Noir S, Colby T, Harzen A, Schmidt J, Panstruga R (2009) A proteomic analysis of powdery mildew (*Blumeria graminis* f.sp. *hordei*) conidiospores. Mol Plant Pathol **10:** 223–236

Oh MH, Moon YH, Lee CH (2003) Increased stability of LHCII by aggregate formation during dark-induced leaf senescence in the Arabidopsis mutant, ore10. Plant Cell Physiol **44:** 1368–1377

Panstruga R (2005) Serpentine plant MLO proteins as entry portals for powdery mildew fungi. Biochem Soc Trans **33:** 389–392

Pesaresi P, Lunde C, Jahns P, Tarantion D, Meurer J, Varotto C, Hirtz RD, Soave C, Scheller HV, Salamini F, et al (2002) A stable LHCII-PSI aggregate and suppression of photosynthetic state transitions in the psae1-1 mutant of Arabidopsis thaliana. Planta **215:** 940–948

Piffanelli P, Zhou FS, Casais C, Orme J, Jarosch B, Schaffrath U, Collins NC, Panstruga R, Schulze-Lefert P (2002) The barley MLO modulator of defense and cell death is responsive to biotic and abiotic stress stimuli. Plant Physiol **129:** 1076–1085

Pruzinská A, Tanner G, Aubry S, Anders I, Moser S, Muller T, Ongania KH, Krautler B, Youn JY, Liljegren SJ, et al (2005) Chlorophyll breakdown in senescent Arabidopsis leaves: characterization of chlorophyll catabolites and of chlorophyll catabolic enzymes involved in the degreening reaction. Plant Physiol **139:** 52–63

Reuber TL, Plotnikova JM, Dewdney J, Rogers EE, Wood W, Ausubel FM (1998) Correlation of defense gene induction defects with powdery mildew susceptibility in *Arabidopsis* enhanced disease susceptibility mutants. Plant J **16:** 473–485

Schenk PM, Kazan K, Rusu AG, Manners JM, Maclean DJ (2005) The *SEN1* gene of Arabidopsis is regulated by signals that link plant defence responses and senescence. Plant Physiol Biochem **43:** 997–1005

Schmelzer E (2002) Cell polarization, a crucial process in fungal defence. Trends Plant Sci **7:** 411–415

Schmid M, Davison TS, Henz SR, Pape UJ, Demar M, Vingron M, Scholkopf B, Weigel D, Lohmann JU (2005) A gene expression map of *Arabidopsis thaliana* development. Nat Genet **37:** 501–506

Schuhegger R, Nafisi M, Mansourova M, Petersen BL, Olsen CE, Svatos A, Halkier BA, Glawischnig E (2006) CYP71B15 (PAD3) catalyzes the final step in camalexin biosynthesis. Plant Physiol **141:** 1248–1254

Skou JP (1982) Callose formation responsible for the powdery mildew resistance in barley with genes in the ml-o locus. J Phytopathol **104:** 90–95

Skou JP (1985) On the enhanced callose deposition in barley with ml-o powdery mildew resistance genes. J Phytopathol **112:** 207–216

Smart MG, Aist JR, Israel HW (1986) Structure and function of wall appositions. 2. Callose and the resistance of oversize papillae to penetration by *Erysiphe graminis* f.sp. *hordei*. Can J Bot **64:** 802–804

Smyth GK (2005) Limma: linear models for microarray data. *In* R Gentleman, V Carey, S Dudoit, R Irizarry, W Huber, eds, Bioinformatics and Computational Biology Solutions Using R and Bioconductor. Springer, New York, pp 397–420

Stein M, Dittgen J, Sanchez-Rodriguez C, Hou BH, Molina A, Schulze-Lefert P, Lipka V, Somerville S (2006) *Arabidopsis* PEN3/PDR8, an ATP binding cassette transporter, contributes to nonhost resistance to inappropriate pathogens that enter by direct penetration. Plant Cell **18:** 731–746

Strain HH, Cope BT, Svec WA (1971) Analytical procedures for the isolation, identification, estimation and investigation of the chlorophylls. Methods Enzymol **23:** 452–476

Thomma B, Eggermont K, Tierens K, Broekaert WF (1999a) Requirement of functional *Ethylene-Insensitive 2* gene for efficient resistance of Arabidopsis to infection by *Botrytis cinerea*. Plant Physiol **121:** 1093–1101

Thomma BPHJ, Eggermont K, Penninckx IAMA, Mauch-Mani B, Vogelsang R, Cammue BPA, Broekaert WF (1998) Separate jasmonate-dependent and salicylate-dependent defense-response pathways in Arabidopsis are essential for resistance to distinct microbial pathogens. Proc Natl Acad Sci USA **95:** 15107–15111

Thomma BPHJ, Nelissen I, Eggermont K, Broekaert WF (1999b) Deficiency in phytoalexin production causes enhanced susceptibility of *Arabidopsis thaliana* to the fungus *Alternaria brassicicola*. Plant J **19:** 163–171

Truman WM, Bennett MH, Turnbull CGN, Grant MR (2010) Arabidopsis auxin mutants are compromised in systemic acquired resistance and exhibit aberrant accumulation of various indolic compounds. Plant Physiol **152:** 1562–1573

Tsuji J, Jackson EP, Gage DA, Hammerschmidt R, Somerville SC (1992) Phytoalexin accumulation in *Arabidopsis thaliana* during the hypersensitive reaction to *Pseudomonas syringae* pv *syringae*. Plant Physiol **98:** 1304–1309

van Baarlen P, Woltering EJ, Staats M, van Kan JAL (2007) Histochemical and genetic analysis of host and non-host interactions of Arabidopsis with three *Botrytis* species: an important role for cell death control. Mol Plant Pathol **8:** 41–54

Varotto C, Pesaresi P, Meurer J, Oelmuller R, Steiner-Lange S, Salamini F, Leister D (2000) Disruption of the Arabidopsis photosystem I gene psaE1 affects photosynthesis and impairs growth. Plant J **22:** 115–124

Vogel J, Somerville S (2000) Isolation and characterization of powdery mildew-resistant *Arabidopsis* mutants. Proc Natl Acad Sci USA **97:** 1897–1902

Weaver LM, Amasino RM (2001) Senescence is induced in individually darkened Arabidopsis leaves but inhibited in whole darkened plants. Plant Physiol **127:** 876–886

Wildermuth MC, Dewdney J, Wu G, Ausubel FM (2001) Isochorismate synthase is required to synthesize salicylic acid for plant defence. Nature **414:** 562–565

Winter D, Vinegar B, Nahal H, Ammar R, Wilson GV, Provart NJ (2007) An "electronic fluorescent pictograph" browser for exploring and analyzing large-scale biological data sets. PLoS One **2:** e718

Wolter M, Hollricher K, Salamini F, Schulze-Lefert P (1993) The *mlo* resistance alleles to powdery mildew infection in barley trigger a

developmentally controlled defense mimic phenotype. Mol Gen Genet **239:** 122–128

Woo HR, Chung KM, Park JH, Oh SA, Ahn T, Hong SH, Jang SK, Nam HG (2001) ORE9, an F-box protein that regulates leaf senescence in *Arabidopsis*. Plant Cell **13:** 1779–1790

Yoshimoto K, Jikumaru Y, Kamiya Y, Kusano M, Consonni C, Panstruga R, Ohsumi Y, Shirasu K (2009) Autophagy negatively regulates cell death by controlling NPR1-dependent salicylic acid signaling during senescence and the innate immune response in *Arabidopsis*. Plant Cell **21:** 2914–2927

Zeyen RJ, Carver TLW, Lyngkaer MF (2002) Epidermal Cell Papillae. American Phytopathological Society, St. Paul

Zhao YD, Hull AK, Gupta NR, Goss KA, Alonso J, Ecker JR, Normanly J, Chory J, Celenza JL (2002) Trp-dependent auxin biosynthesis in *Arabidopsis*: involvement of cytochrome P450s CYP79B2 and CYP79B3. Genes Dev **16:** 3100–3112

Zhou N, Tootle TL, Glazebrook J (1999) *Arabidopsis PAD3*, a gene required for camalexin biosynthesis, encodes a putative cytochrome P450 monooxygenase. Plant Cell **11:** 2419–2428